Constrained TCRγδ-associated Syk activity engages PI3K to facilitate thymic development of IL-17A–secreting γδ T cells

Nital Sumaria, Stefania Martin and Daniel J. Pennington*

Blizard Institute, Barts and The London School of Medicine and Dentistry, Queen Mary University of London, 4 Newark Street, London, E1 2AT, UK.

*Corresponding author. Email: d.pennington@qmul.ac.uk (D.J.P)

ABSTRACT

Murine γδ^{17} cells, which are T cells that bear the γδ T cell receptor (TCRγδ) and secrete interleukin-17A (IL-17A), are generated in the thymus and are critical for various immune responses. Although strong TCRγδ signals are required for the development of interferon-γ (IFN-γ)-secreting γδ cells (γδ^{IFN} cells), the generation of γδ^{17} cells requires weaker TCRγδ signaling. Here, we demonstrated that constrained activation of the kinase Syk downstream of TCRγδ was required for the thymic development of γδ^{17} cells. Increasing or decreasing Syk activity by stimulating TCRγδ or inhibiting Syk, respectively, substantially reduced γδ^{17} cell numbers. This delimited Syk activity optimally engaged the phosphoinositide 3-kinase (PI3K)-Akt signaling pathway, which maintained the expression of master regulators of the IL-17 program, RORγt and c-Maf. Inhibition of PI3K not only abrogated γδ^{17} cell development, but also augmented the development of a distinct, previously undescribed subset of γδ T cells. These CD8^{+}Ly6a^{+} γδ T cells had a type-I interferon gene expression signature and expanded in response to stimulation with IFN-β. Collectively, these studies elucidate how weaker TCRγδ signaling engages distinct signaling pathways to specify the γδ^{17} cell fate and identifies a role for type-I interferons in γδ T cell development.

INTRODUCTION

T cells bearing T cell receptors (TCRs) composed of γ and δ chains, γδ T cells, respond rapidly to an array of pathogens that includes human immunodeficiency virus (HIV) [1], influenza viruses [2], malaria parasites [3] and *Mycobacterium tuberculosis* [4]. Moreover, they are implicated in immunopathologies such as psoriasis [5] and multiple sclerosis [6] and possess anti-tumour properties [7]. Instrumental to this early involvement in host defense is their production of cytokines that mediate direct effector functions and help instruct appropriate downstream activation of adaptive lymphocytes. For example, γδ T cell–associated cytotoxic and anti-tumour responses correlate with secretion of interferon γ (IFNγ) [8], whereas secretion of interleukin 17A (IL-17A) orchestrates coordinated engagement of immune responses to bacterial and fungal infections [9, 10].

Unlike αβ T cells, which adopt cytokine-secreting effector functions only when required to participate in ongoing immune responses, γδ T cells instead commit to subsequent effector fate (the secretion of IL-17 or IFNγ) during their development in the thymus [11, 12]. γδ T cells are thought to diverge from a common (αβ/γδ) thymocyte progenitor at the early $CD4^-CD8^-$ "double negative" (DN) stage of differentiation, instructed by strong (akin to TCR cross-linking) TCR signaling from recently rearranged and expressed TCRγδ complexes [13-15]. It is at this point that γδ progenitors commit to subsequent effector fate, although the mechanisms that drive this process are not fully understood.

We and others have provided clear evidence that thymic TCRγδ signaling plays a central role in determining γδ T cell effector fate [16-22]. A consistent message from these studies is that strong TCRγδ signals drive γδ progenitors toward an IFNγ-secreting ($γδ^{IFN}$) fate but are prohibitive for development of IL-17–committed γδ T ($γδ^{17}$) cells. This presents an obvious conundrum: How do $γδ^{17}$ cells develop if the strong TCRγδ signals required for DN thymocyte commitment to the γδ lineage are subsequently prohibitive to their generation? Our ongoing work seeks to address this key issue by exploring the differential signaling inputs that govern the development of the $γδ^{17}$ and $γδ^{IFN}$ cell lineages. Indeed, to this end we have demonstrated that engagement of the extracellular signal–regulated kinase (ERK) mitogen-activated protein kinase (MAPK) pathway downstream of TCRγδ favoured the development of $γδ^{IFN}$ cells but not $γδ^{17}$ cells [20].

Here, we demonstrated that TCRγδ-associated activity of the tyrosine kinase Syk is necessary to engage the phosphoinositide 3-kinase (PI3K) and Akt signaling pathway to facilitate $γδ^{17}$ cell

development in mice. Crucially, however, this requirement for Syk is constrained, because either an increase or a decrease in Syk activity attenuated the generation of $\gamma\delta^{17}$ cells. In the absence of appropriate Syk-PI3K-Akt signaling, expression of key master regulator genes of the IL-17 program, such as *Rorc* and *Maf*, was significantly reduced on a per-cell basis. Impairment of PI3K signaling in $\gamma\delta$ progenitors also resulted in the unanticipated adoption of a type-I interferon gene signature that identifies a previously unknown innate-like $CD8^{+}Ly6a^{+}$ $\gamma\delta$ T cell subset. Collectively, these data mechanistically link the requirement for "weak" TCR$\gamma\delta$ signaling to a distinct signaling modality for generation of $\gamma\delta^{17}$ cells, and identify a novel role for type-I interferons in development of $\gamma\delta$ T cells.

RESULTS

Development of $\gamma\delta^{17}$ cells requires constrained Syk activity

Although our previous work had shown that strong signaling through TCR$\gamma\delta$ is not compatible with thymic development of $\gamma\delta^{17}$ cells [20], the extent to which TCR$\gamma\delta$ signaling pathways are actually required for generation of $\gamma\delta^{17}$ cells remained unclear. All TCR signaling requires proximal tyrosine kinase activity to initiate signal transduction. Thus, we assessed by flow cytometry the presence of the kinases Lck, Zap70, and Syk in developing $\gamma\delta$ progenitors from wild-type (WT) embryonic day 15 (E15) thymic lobes that had been allowed to develop for 7 days in fetal thymic organ culture (FTOC). FTOC faithfully reproduces T cell development in vitro [23] and is ideal for studying the perinatal development of $\gamma\delta$ T cells, in which early $CD24^{+}$ ($\gamma\delta^{24+}$) progenitors progress to a $CD24^{-}CD44^{-}CD45RB^{-}$ triple-negative ($\gamma\delta^{TN}$) stage before either becoming $CD45RB^{+}$ ($\gamma\delta^{RB}$ cells) — and in some cases then also $CD44^{+}$ ($\gamma\delta^{IFN}$ cells) — in an IFNγ-secreting developmental pathway, or becoming $CD44^{+}CD45RB^{-}$ ($\gamma\delta^{17}$ cells) in an IL-17–secreting developmental pathway (**fig. S1**) [20].

Intracellular flow cytometry revealed that both Lck and Zap70 were present at only low levels in $\gamma\delta^{24+}$ progenitors (**Fig. 1A**). By contrast, Syk abundance was highest in $\gamma\delta^{24+}$ cells. The presence of Syk and Zap70 was not strictly mutually exclusive (**fig. S2A**), but was similar between all $\gamma\delta$ T cell subsets expressing distinct TCRγ-chain variable regions (Vγ) that were tested (**fig. S2B**). These data are consistent with previous reports that Syk is a dominant kinase at the β-selection checkpoint [24], whereas Zap70 dominates in mature peripheral cells. We confirmed this in splenic $\gamma\delta$ T cells in which only Zap70, but not Syk, was present (**fig. S2C**). Phosphorylated Syk was detected in all thymic $\gamma\delta$ cell subsets but was particularly evident in cells of the IFNγ

developmental pathway, consistent with these cells receiving stronger TCRγδ signals than do $\gamma\delta^{17}$ cells (**fig. S2D**).

Because Syk appears to be the dominant TCR downstream tyrosine kinase in early γδ progenitors, we next assessed whether some amount of Syk activity (and by inference TCRγδ signaling), was necessary for $\gamma\delta^{17}$ cell development by placing WT E15 thymic lobes in 7-day FTOC in the presence of increasing concentrations of the Syk inhibitor BAY-61-3606 [25], which reduces Syk phosphorylation in a dose-dependent manner (**Fig. 1B**). Compared to control conditions, inhibition of Syk resulted in a marked decrease in the generation of $\gamma\delta^{17}$ cells (**Fig. 1C**). Under conditions of partial Syk blockade (0.4μM BAY-61-3606), increased signaling through TCRγδ, induced by the addition of the activating TCRδ-specific antibody GL3, rescued the generation of $\gamma\delta^{17}$ cells (**Fig. 1D, and fig. S2E**), revealing an antagonistic relationship between Syk inhibition and TCRγδ stimulation. Nonetheless, as the concentration of GL3 was increased, thereby stimulating more TCRγδ signaling, the generation of $\gamma\delta^{17}$ cells was again markedly reduced (**Fig. 1D**). Thus, these data suggest that delimited Syk activity is required for efficient generation of $\gamma\delta^{17}$ cells from γδ progenitors.

Generation of $\gamma\delta^{17}$ cells requires PI3K activity

We next considered that this delimited Syk activity must activate a distinct downstream signaling pathway to promote $\gamma\delta^{17}$ cell development. A likely candidate was the PI3K pathway, because PI3Kδ-deficient mice had previously been reported to be resistant to psoriasis induction due to the absence of $\gamma\delta^{17}$ cells [26]. To investigate, we assessed peripheral γδ T cell compartments in PI3Kδ-deficient (*p110δ*$^{-/-}$) animals. Adult *p110δ*$^{-/-}$ mice had significantly reduced numbers of $\gamma\delta^{17}$ cells in peripheral lymph nodes (LN) compared to controls (**Fig. 2A** and **fig. S3**). To assess thymic development, E15 thymic lobes from PI3Kδ-deficient animals were cultured in FTOC for 7 days. Consistent with the reduced number of $\gamma\delta^{17}$ cells in the LNs of PI3Kδ-deficient mice, thymic lobes from these animals generated substantially fewer $\gamma\delta^{17}$ cells than did WT controls (**Fig. 2B**), and this reduction in cell number was not a consequence of altered proliferation (**fig. S4A**) or apoptosis (**fig. S4B**). Culturing thymic lobes from *p110δ*$^{-/-}$ embryos for 14 days to allow for the generation of both γ-chain variable region 6 ($V\gamma6^{+}$)-expressing $\gamma\delta^{17}$ cells, which develop in an initial wave, and the subsequent development of $V\gamma6^{-}$ $\gamma\delta^{17}$ cells, demonstrated that all $\gamma\delta^{17}$ subsets, regardless of Vγ-usage, required PI3Kδ for efficient development (**Fig. 2C**). This requirement for PI3Kδ was cell-intrinsic, because E15 thymocytes purified from PI3Kδ-deficient animals showed comparable developmental defects when cultured on PI3K-sufficent OP9-DL1 stromal cells [27] (**Fig. 2D**).

The class I family of PI3K consists of four members: the class Ia PI3Kα, PI3Kβ, and PI3Kδ, and the class Ib PI3Kγ [28]. Specific inhibitors of PI3Kα, PI3Kβ, or PI3Kγ had marginal effects on γδ T cell development in E15 7-day FTOC of WT thymic lobes (**fig. S5A**). By contrast, specific inhibition of PI3Kδ or pan-inhibition of all class I PI3Ks recapitulated the significant reduction of $\gamma\delta^{17}$ cell development observed in E15 FTOC of thymic lobes from *p110δ*$^{-/-}$ mice (**fig. S5, A and B**). Inhibition of Akt (also called protein kinase B), a major downstream target of PI3K, also strongly reduced $\gamma\delta^{17}$ cell generation **(Fig. 2E).** The use of FTOC additionally allowed for pharmacological inhibition of phosphatase and tensin homolog (PTEN), which negatively regulates PI3K activity [28]. As expected, PTEN inhibition in 7-day FTOC of WT thymic lobes resulted in a significant increase in the development of $\gamma\delta^{17}$ cells (**Fig. 2F**). Consistent with this, 7-day FTOC of E15 thymic lobes from *p110δ*^{E1020K} knock-in mice, which have an activating mutation in the p110 catalytic subunit of PI3Kδ [29], also generated significantly increased numbers of $\gamma\delta^{17}$ cells (**Fig. 2G**). This was also reflected in increased numbers of $\gamma\delta^{17}$ cells in peripheral lymph nodes of adult *p110δ*^{E1020K} mice compared to littermate controls (**Fig. 2H**). Thus, activation of the PI3K signaling pathway is a key requirement for thymic development of all $\gamma\delta^{17}$ cell subsets.

TCRγδ-associated Syk activity engages PI3K signaling

We next explored the relationship between TCR-associated Syk activity and the activation of PI3K signaling, both of which were required for development of $\gamma\delta^{17}$ cells. To do this, we treated E15 thymic lobes from WT embryos with inhibitors of either PI3K or Syk for 1 day and then harvested, fixed, and assessed γδ T cells for intracellular phosphorylated Akt (pAkt) as a readout of activation of the PI3K pathway. As expected, PI3K blockade resulted in reduced pAkt compared to controls (**Fig. 3A**). A reduction in pAkt was also observed in γδ progenitors in thymic lobes treated with Syk inhibitor (**Fig. 3A**), suggesting that Syk activity is required for activation of the PI3K-Akt pathway.

These data suggested a model in which constrained TCRγδ-associated Syk activity stimulates PI3K for optimal development of $\gamma\delta^{17}$ cells. Such a model predicts that increasing Syk activity above this optimal range, for example by TCRγδ stimulation with GL3, would not rescue partial inhibition of PI3K but would instead augment PI3K inhibition. To test this, we placed WT thymic lobes in 7-day FTOC with partial PI3K inhibition (0.25μM ZSTK474, the pan-PI3K inhibitor) and increasing concentrations of GL3. Note that partial inhibition of PI3K resulted in a significant reduction in the generation of $\gamma\delta^{17}$ cells but did not block it completely (**fig. S5B**). As predicted, increased TCRγδ signaling exacerbated PI3K-mediated inhibition of $\gamma\delta^{17}$ cell development to the

point that the generation of these cells effectively ceased completely (**Fig. 3B**). This synergistic effect was also observed in 7-day FTOC of *p110δ*$^{-/-}$ thymic lobes treated with increasing concentrations of GL3 (**fig. S6**).

This model also predicts that direct activation of PI3K should overcome the negative effects of Syk blockade on $\gamma\delta^{17}$ cell development. To test this, we added the PTEN inhibitor SF1670, which indirectly activates PI3K, to 7-day FTOC of WT thymic lobes in the presence of partial Syk inhibition. As predicted, addition of the PTEN inhibitor rescued $\gamma\delta^{17}$ cell development in the presence of the Syk inhibitor (**Fig. 3C**). Moreover, PTEN inhibition also rescued the generation of $\gamma\delta^{17}$ cells in the presence of the TCRδ-activating antibody GL3 (**Fig. 3D**), demonstrating that augmented PI3K activity overrides the negative effects on $\gamma\delta^{17}$ cell development of manipulating Syk activity, either positively or negatively, beyond an optimal range. These data suggested that greater TCRγδ-associated Syk activity, such as that induced by GL3 (**Fig. 3E**), may also reduce PI3K activation. Consistent with this, a small but significant reduction in PI3K-AKT activity, as indicated by a reduction in ribosomal protein S6 phosphorylation (pS6), in $\gamma\delta^{24+}$ cells was observed in response to GL3 (**Fig. 3F**). However, this GL3-induced decrease in PI3K-AKT activity was less than that observed when we inhibited Syk (**Fig. 3F**). Thus, the effect of increased Syk activity on reduced $\gamma\delta^{17}$ cell development may also be through mechanisms independent of the observed reduction in PI3K signaling. Indeed, we have previously shown that TCRγδ-mediated ERK activation inhibits $\gamma\delta^{17}$ cell development [20]. However, inhibition of ERK, which would normally increase $\gamma\delta^{17}$ cell number [20], did not rescue $\gamma\delta^{17}$ cell development in the presence of PI3K or Syk inhibition (**Fig. 3G**). This highlights the importance of the Syk-PI3K axis, because, although increased PI3K activity can overcome the inhibitory effect of TCRγδ-mediated ERK activation on $\gamma\delta^{17}$ cell development (**Fig. 3D**), the reverse is not true: ERK inhibition cannot overcome a deficit in Syk-PI3K signaling.

The activation of PI3K is also associated with cytokine signaling [30]. $\gamma\delta^{17}$ cells express both the IL-1 receptor (IL-1R) and the IL-7 receptor (IL-7R) (**fig. S7A**), and expand considerably in absolute number when either IL-1β or IL-7 are added to 7-day FTOC of WT thymic lobes (**fig. S7B**) [31]. Thus, we assessed whether IL-1β or IL-7 could activate PI3K in the context of $\gamma\delta^{17}$ cell development. Given that a PTEN inhibition–induced increase of PI3K activity rescued the generation of $\gamma\delta^{17}$ cells in the presence of Syk blockade (**Fig. 3C**), we assessed whether the addition of either IL-1β or IL-7 could also increase PI3K activity to rescue $\gamma\delta^{17}$ cell development under conditions of Syk inhibition. However, the addition of IL-1β or IL-7 to 7-day FTOC of WT thymic lobes in the presence of partial Syk blockade failed to significantly increase the generation of $\gamma\delta^{17}$ cells (**Fig. 3H**), suggesting that neither IL-1β nor IL-7 were capable of

stimulating PI3K activity downstream of Syk. Collectively, these data are consistent with a model in which delimited TCRγδ-associated Syk activity can optimally activate PI3K-Akt signaling to promote thymic $\gamma\delta^{17}$ cell development.

PI3K inhibition reveals a distinct γδ T cell transcriptional program

To further interrogate the role of PI3K signaling in early γδ T cell development, we next assessed gene expression, using single-cell RNA sequencing (scRNA-seq), in γδ progenitors that had developed in 8-day FTOC of WT E15 thymic lobes in the presence or absence of PI3K inhibition (**Fig. 4A**). We found that γδ T cells from PI3K inhibitor–treated FTOC predominantly clustered separately from their control counterparts (**Fig. 4A**). Expression of *Il2ra* (CD25), *Cd24a*, *Cd44*, *Cd27*, *Klrb1c* (NK1.1), and *Il2rb* (CD122), plus assessment of Vγ-usage, allowed demarcation of $\gamma\delta^{17}$ cells, $\gamma\delta^{IFN}$ cells, and a grouping of more immature subsets consisting of $\gamma\delta^{24+}$, $\gamma\delta^{TN}$, and $\gamma\delta^{RB}$ cells (**fig. S8, A** to **C**). The expression of genes associated with an IL-17–secreting program, such as *Maf*, *Rorc*, *Blk*, *Il23r*, and *Sox13*, further confirmed the $\gamma\delta^{17}$ cluster (**Fig. 4B**). As shown above, the development of γδ progenitors along the IL-17 developmental pathway was substantially reduced in the presence of PI3K inhibition (**Fig. 4A**). Gene expression analysis of PI3K inhibitor–treated γδ T cells that did segregate with untreated $\gamma\delta^{17}$ cells showed markedly reduced expression of genes known to associate with a $\gamma\delta^{17}$-specific signature, such as *Cd163l1* (Scart1), *Blk*, *Maf*, and *Sox13* [32] (**Fig. 4C**).

We also observed expansion of $\gamma\delta^{RB}$ cells (and to some extent $\gamma\delta^{TN}$ cells) in 7-day FTOC of WT thymic lobes treated with PI3K inhibitor (**Fig. 4A**), which was also evident in 7-day FTOC of thymic lobes from *p110δ*$^{-/-}$ mice (**Fig. 2B**), and in adult PI3Kδ-deficient mice (**fig. S3**). These expanded cells displayed an expression signature characterised by increased expression of host defense genes (**Fig. 4D** and **fig. S8D**). Gene ontology and enrichment pathway analysis using Metascape [33] showed that this signature was heavily enriched for genes associated with interferon signaling, particularly type-I interferon signaling (**Fig. 4E**). A feature of this signature was an increase in expression of both *Cd8b1* and *Ly6a* (**Fig 4D**). Analysis of single cells from untreated 8-day FTOC of WT thymic lobes revealed two clusters (#2 and #6) in which *Cd8b1* and *Ly6a* expression was evident (**Fig. 4F**). Cells of cluster #6 displayed the prominent interferon signaling signature (**fig. S8E**), whereas those in cluster #2 displayed features of thymically-derived innate T cells (**fig. S8F**) [34]. $CD8\beta^{+}Ly6a^{+}$ γδ T cells were readily identified by flow cytometry from WT thymic lobes and expanded in response to IFN-β treatment in 7-day FTOC (**Fig. 4G**) or inhibition of PI3K in 5-day FTOC (**fig. S8G**). Moreover, under conditions of

PI3K inhibition, non-$\gamma\delta^{17}$ cells made significantly more IFNγ compared to similar cells from untreated lobes, consistent with a more innate-like phenotype (**fig. S8H**).

The importance of this heretofore unreported $\gamma\delta$ T cell–associated type-I interferon gene signature and the expansion of a previously undescribed innate-like CD8β^{+}Ly6a^{+} $\gamma\delta$ T cell subset in the presence of IFN-β, both of which were suppressed by PI3K-Akt signaling, will require further investigation and lies outside the scope of the current study. Nonetheless, the increase in cells exhibiting such a profile upon PI3K inhibition may be linked to increased activity of the transcription factor Foxo1, because PI3K signaling negatively regulates Foxo1 by facilitating its nuclear export and degradation [35]. Consistent with this, imagestream analysis of $\gamma\delta^{IFN}$ cells from PI3K inhibitor–treated thymic lobes showed increased nuclear localization of Foxo1 and significant increase in expression of Foxo1 target genes, such as *Sell* (CD62L), *Klf2*, *S1pr1*, and *Ccr7* (**fig. S9, A to C**). In addition, IL-7Rα, which is critical for appropriate $\gamma\delta$ T cell development and is a well-characterized target of Foxo1 transcriptional activity, showed a significant increase in abundance on non-$\gamma\delta^{17}$ cells from PI3K inhibitor–treated lobes (**fig. S9D**). Notably, treatment of WT lobes with either Syk inhibitor or GL3, both of which we propose push Syk activity beyond an optimal range for $\gamma\delta^{17}$ cell development, also increased IL-7Rα on non-$\gamma\delta^{17}$ cells (**fig. S9D**), further supporting a link between constrained TCR$\gamma\delta$-associated Syk activity and the PI3K-Akt pathway in developing $\gamma\delta$ progenitors.

Impairment of Syk-PI3K signaling attenuates expression of RORγt and c-Maf in developing $\gamma\delta$ progenitors

The scRNA-seq data suggested that a mechanism by which PI3K inhibition might lead to decreased generation of $\gamma\delta^{17}$ cells was through reduced expression of key master regulator genes of the IL-17-program, such as *Rorc* and *Maf*, both of which are highly expressed in $\gamma\delta^{17}$ cells (**Fig. 4B** and **fig. S10, A and B**) [17, 36]. To confirm, E15 thymic lobes from *Rorc(γt)*$^{+/GFP}$ mice, which express green fluorescent protein (GFP) from the RAR-related orphan receptor gamma-t (RORγt) promoter were cultured for 6 days in the presence or absence of PI3K inhibitor. Inhibition of PI3K reduced the frequency of RORγt^{+} $\gamma\delta^{24+/TN}$ progenitors (**Fig. 5A**), and the RORγt^{+} $\gamma\delta^{24+/TN}$ progenitors that were present had much lower amounts of RORγt on a per-cell basis when PI3K signaling was impaired (**Fig. 5A**). A similar significant reduction in RORγt in $\gamma\delta^{24+/TN}$ progenitors was also observed when E15 thymic lobes from *Rorc(γt)*$^{+/GFP}$ mice were cultured with either Syk inhibitor (**Fig. 5B**), or activating antibody GL3 (**Fig. 5C**), which reduce or increase proximal TCR$\gamma\delta$–associated Syk activity, respectively. The abundance of c-Maf was

also assessed under these conditions. Similar to RORγt, the frequency of c-Maf^{+} γδ$^{24+/TN}$ progenitors, and the amount of c-Maf on a per-cell basis were both significantly reduced when WT E15 thymic lobes were cultured in the presence of PI3K inhibitor, Syk inhibitor, or GL3 antibody (**Fig. 5D**). Collectively, these data suggest that constrained TCRγδ-associated Syk activity is required to activate the PI3K-Akt pathway in early γδ progenitors to maintain the expression of key master regulator transcription factors associated with IL-17 secretion and establishment of a γδ^{17} cell fate.

DISCUSSION

Consensus suggests that to enter the γδ T cell lineage DN thymocytes must express a surface T cell receptor complex with the capacity to transduce a "strong" TCR signal [13-15]. Essentially this is mediated by TCRγδ that, by nature of its high surface abundance, signals at significantly higher amounts than does the competing preTCR (pTα paired with TCRβ) that instead instructs DN progenitors toward the αβ T cell lineage. After entering the γδ lineage, thymic γδ progenitors further commit to subsequent effector fate, mainly to express either IFNγ or IL-17. TCRγδ signal strength is implicated here too, with strong TCRγδ signaling promoting an IFNγ-secreting fate and only weaker TCRγδ signaling being compatible with the generation of γδ^{17} cells [16-20]. However, the signaling modalities that manifest these weaker TCRγδ signals and the conceptual challenge of explaining the paradoxical requirement for both strong (to commit to the lineage) and weak (to commit to effector function) TCRγδ signals to adopt a γδ^{17} cell fate, have remained essentially unresolved.

This study begins to address these issues. We demonstrated that constrained activity of the TCR-proximal kinase Syk was required for γδ^{17} cell development. Syk inhibition or increased TCRγδ signaling acted antagonistically to decrease or increase, respectively, Syk activity beyond an optimal range for the generation of γδ^{17} cells. Optimal Syk activity, in turn, engaged the PI3K-Akt pathway that is necessary for appropriate maintenance of the IL-17-secreting program master regulators, RORγt and c-Maf. These data directly contradict a previous study that suggested a positive correlation between TCRγδ stimulation, Syk phosphorylation, and PI3K activation in thymic γδ progenitors [37]. Such a model would predict that TCRγδ stimulation (such as with the activating antibody GL3) should rescue partial pharmacological inhibition of PI3K for the development of γδ^{17} cells. However, our data demonstrate exactly the opposite, with the combination of TCRγδ stimulation and partial PI3K inhibition instead being additive and

negative. Indeed, our findings explain how "weaker" TCRγδ signaling translates to distinct signaling modalities that permit certain γδ progenitors to adopt the $\gamma\delta^{17}$ cell fate.

These findings have important implications for the nature of $\gamma\delta^{17}$-associated TCRs – specifically, that characteristics of $\gamma\delta^{17}$-associated TCRs must restrict TCR signaling to permit Syk-mediated engagement of PI3K-Akt signaling that promotes a $\gamma\delta^{17}$ cell phenotype. An obvious modulator of TCR signaling is TCR-ligand engagement. For example, increased signaling mediated by a Skint1-associated TCR-ligand for the Vγ5Vδ1^{+}TCR has been implicated in the development of Vγ5^{+} progenitors along the CD45RB^{+} IFNγ-pathway [18]. Moreover, in KN6 transgenic mice (which express a single Vγ4Vδ5^{+}TCR), on a recombination-activating gene (RAG)-deficient background, thymic provision of the high-affinity ligand H2-T22 (an MHC class-Ib molecule) promotes $\gamma\delta^{IFN}$ cell development, whereas presence of the lower affinity ligand H2-T10 permits some generation of $\gamma\delta^{17}$ cells, possibly through assistance from Notch signaling and cytokines such as IL-1β, IL-21 and IL-23 [21, 38]. Nonetheless, in the absence of identified ligands for the vast majority of murine TCRγδ, other explanations for TCR signal modulation must also be considered [12]. Thus, a constrained TCRγδ signal strength may also be a consequence of certain TCRγ-TCRδ pairings that do not allow the formation of fully signaling-competent TCR-CD3 complexes. Alternatively, factors that are co-expressed in the perinatal period, during which all $\gamma\delta^{17}$ cells develop [39], may interact with certain TCRγδ to constrain signaling. Possible candidates for these putative signal-modulating factors could be members of the group B scavenger receptor cysteine-rich (SRCR) family of proteins. These include SCART1 (CD163L1) and SCART2 (5830411N06Rik) that are predominantly expressed on Vγ6^{+} and Vγ4^{+} $\gamma\delta^{17}$ cells, respectively [32, 40]. Notably, the SRCR family WC1 proteins, which are closely related to SCART1 and SCART2, are known to form complexes with TCRγδ on bovine γδ T cells [41]. These interactions appear to alter the signaling capacities of the TCR by providing additional intracellular docking sites for kinase binding. Thus, it is conceivable that comparable interactions between $\gamma\delta^{17}$-associated TCRs and SCART1 or SCART2 may modulate intracellular signaling to promote Syk-PI3K-Akt–mediated $\gamma\delta^{17}$ cell development, an idea that we are currently exploring.

A modulated or constrained TCRγδ signal that permits engagement of Syk-PI3K-Akt to promote $\gamma\delta^{17}$ cell development does not in itself satisfactorily address the paradoxical requirement for a "weaker-signaling" $\gamma\delta^{17}$-associated TCRγδ to have first signalled strongly enough to commit a DN progenitor to the γδ lineage [12]. This raises the intriguing possibility that distinct $\gamma\delta^{17}$ progenitors might exist that possess different developmental potentials compared with the

conventional DN progenitors that enter either the αβ or $\gamma\delta^{IFN}$ lineages as a consequence of weaker or stronger signaling, respectively, at the β-selection checkpoint [42]. Thus, constrained TCRγδ signaling that engages the Syk-PI3K-Akt pathway in a putative $\gamma\delta^{17}$ progenitor would be compatible with continued development toward a $\gamma\delta^{17}$ cell phenotype that shares many similarities with RORγt$^+$ type 3 innate lymphoid cells (ILC3) and especially lymphoid tissue inducer (LTi) cells [43, 44]. By contrast, stronger conventional TCRγδ signaling that also engages alternative downstream signaling pathways, such as ERK, may be incompatible with the continued development of these alternative $\gamma\delta^{17}$ progenitors [20].

The possible existence of separate $\gamma\delta^{17}$ progenitors is supported by studies from two groups. Shibata and colleagues suggested that although $\gamma\delta^{IFN}$ cells could be generated (like αβ T cells) from both DN2 and DN3 thymocyte progenitors, $\gamma\delta^{17}$ cells could develop only from c-kit^{hi} DN2 cells [45]. Similarly, a prior report from the Kang group had also suggested that c-kit$^+$ "early thymic progenitors" were a source of $\gamma\delta^{17}$ cells, but were restricted to generating only the Vγ4$^+$ subset [46]. Unlike other $\gamma\delta^{17}$ subsets, Vγ4$^+$ $\gamma\delta^{17}$ cells appear to require Sox4 and Sox13 for development [46, 47]. Moreover, the transcriptional signature of immature CD24$^+$Vγ4$^+$ cells segregated from other immature γδ T cell subsets in a principle components analysis of microarray-derived transcriptomic data [46]. Somewhat surprisingly, a follow-up study re-characterized the putative Vγ4$^+$ $\gamma\delta^{17}$ progenitors as c-kit$^-$ (rather than c-kit$^+$), CD24$^+$ DN1 (DN1d) cells that were also Sox13$^+$ (so-called "Soxpro" cells) [48]. These Soxpro cells already expressed genes associated with a $\gamma\delta^{17}$ cell program, such as *Maf*, *Rorc*, and *Blk*. They also appeared to favour initiation of Vγ4-targeted TCRγ chain rearrangements and developed as Vγ4$^+$ $\gamma\delta^{17}$ cells when placed in thymic organ culture. Notably however, this study also demonstrated that TCRγδ was still required for differentiation of Soxpro cells into Vγ4$^+$ $\gamma\delta^{17}$ cells, because DN1d cells (including Soxpro cells) accumulated in TCRδ-deficient mice, and DN1d cells from KN6 transgenic mice generated more Vγ4$^+$ $\gamma\delta^{17}$ cells than did control DN1d cells, suggesting that in-frame Vγ4$^+$ TCR rearrangements are normally limiting in the latter. Our data here suggest that this TCRγδ requirement would equate to constrained TCRγδ-associated Syk activity that allows engagement of PI3K-Akt signaling to support the development of $\gamma\delta^{17}$ progenitors to a mature $\gamma\delta^{17}$ cell phenotype. Our findings would also assert that increased TCRγδ signal strength in this Vγ4$^+$ $\gamma\delta^{17}$ progenitor, for example in the presence of the activating antibody GL3, would be incompatible with continued development toward a $\gamma\delta^{17}$ cell phenotype [20].

Although compelling, the focus on a pre-committed progenitor for V$\gamma4^+$ $\gamma\delta^{17}$ cells somewhat ignores the developmental origins of other $\gamma\delta^{17}$ cells, especially the V$\gamma6^+$ $\gamma\delta^{17}$ cells that are generated in a first wave of T cell development alongside V$\gamma5^+$ dendritic epidermal T cell (DETC) progenitors, and that populate diverse body sites such as the female reproductive tract, dermis, and peritoneal and oral cavities [12]. Our data suggest that all $\gamma\delta^{17}$ subsets, regardless of Vγ-usage, require constrained TCR-mediated Syk activity to activate the PI3K-Akt pathway. Thus, all $\gamma\delta^{17}$ subsets may derive from separate precursors that are distinct from conventional $\alpha\beta/\gamma\delta^{IFN}$ progenitors.

Finally, an unanticipated finding from these studies was that inhibition of PI3K signaling in developing $\gamma\delta$ progenitors induced a robust type-I interferon gene signature, particularly in cells of the IFNγ-secreting developmental pathway. This signature has not been previously reported in $\gamma\delta$ T cells and clearly warrants further in-depth investigation. Type-I interferons are expressed in the thymus [49], in which they are suggested to regulate the maturation of conventional $\alpha\beta$ T cells [50]. Thymic type-I interferons have also been suggested to drive development of innate unconventional memory-like CD44$^+$CD8$^+$ T cells in an Eomesodermin-dependent manner [34]. We observed that addition of type-I interferons to WT FTOC promoted the generation of a population of CD8$^+$ $\gamma\delta$ T cells that additionally express Ly6a. Further investigation is underway to understand the functional potential of these cells and their relationship to other innate-like T cell subsets that are also generated in the thymus.

The importance of type-I interferon signaling to $\gamma\delta$ T cell function is not well documented. However, studies have reported expansion of IL-17–secreting $\gamma\delta^{17}$ cells in type-I interferon receptor (IFNAR) knockout mice both in response to *Francisella tularensis* and *Listeria monocytogenes* infections [51] and in a model of secondary *Streptococcus pneumoniae* infection after influenza infection [52]. At least some of the effect of type-I interferon on $\gamma\delta^{17}$ cells was direct, possibly through decreasing the expression of *Rorc* [51]. Nonetheless, there may also be indirect effects through the production of IL-27, which suppresses IL-17 secretion by $\gamma\delta^{17}$ cells [51]. Moreover, type-I interferons are also reported to inhibit the production of IL-1β [53], which is required for expansion of $\gamma\delta^{17}$ cells. Notably, type-I interferons have been reported to have anti-inflammatory properties in autoimmune disease settings, in which IL-17-associated immune responses tend to dominate. Thus, a better understanding of how PI3K signaling regulates the responsiveness to type-I interferons in developing $\gamma\delta$ T cells may provide critical insight into the opposing functions of pro-inflammatory IL-17–driven antibacterial immunity and innate type-I interferon–driven antiviral responses.

MATERIALS AND METHODS

Mice

C57BL/6 wild-type (WT) mice were purchased from Charles River Laboratories. PI3Kδ-deficient mice (*p110δ*$^{-/-}$) [54] and PI3Kδ-hyperactive mice (*p110δ*^{E1020K}) [29] were kindly provided by Prof K Okkenhaug (Cambridge, UK). *Rorc(γt)*$^{+/GFP}$ reporter mice [55] were kindly provided by Dr G Eberl (Pasteur Institute, Paris). All strains were on a C57BL/6 background. Mice were foetal (E15-E17), neonatal (3-4 days) or adult females (4-12 weeks). Embryos were from timed pregnancies. Mice were bred and maintained in specific pathogen-free animal facilities at Queen Mary University of London or relevant facility. All experiments involving animals were performed in full compliance with UK Home Office regulations and institutional guidelines.

Foetal Thymic Organ Cultures (FTOC)

Foetal thymic lobes from WT, *p110δ*$^{-/-}$, *p110δ*^{E1020K}, or *Rorc(γt)*$^{+/GFP}$ mice were cultured on nucleopore membrane filter discs (Whatman) in complete medium (RPMI-1640 with 10% FCS, 1% penicillin and streptomycin, 50 μM β-mercaptoethanol, and 2 mM L-glutamine) for indicated length of time (hours or days). In some experiments the following antibody (eBioscience), inhibitors (Selleckchem), or recombinant cytokines were added to the cultures (concentrations indicated): TCRδ-specific antibody GL3, pan-Akt inhibitor MK-2206, MEK1/2 inhibitor UO126 (Sigma-Aldrich), pan-PI3K inhibitor ZSTK474, p110α inhibitor A66, p110β inhibitor TGX-221, p110δ inhibitor IC87114, p110γ inhibitor AS605240, PTEN inhibitor SF1670, Syk inhibitor BAY-61-3606, interleukin-1β (IL-1β; R&D), IL-7 (Peprotech) and IFN-β (Peprotech). Cultures containing antibody or inhibitors were rested overnight in fresh complete medium before analysis, unless otherwise indicated. All thymic organ cultures were subsequently analysed by flow cytometry.

Tissue processing and cell isolation

Single-cell suspensions of foetal and neonatal thymocytes were obtained by gently homogenizing thymic lobes followed by straining through a 30 μm nylon gauze (Sefar Ltd., UK). To obtain single-cell suspensions of lymphocytes, adult peripheral lymph nodes (axillary, inguinal and brachial) and spleens were teased apart, followed by filtering through an 80 μm stainless steel mesh (Sefar Ltd., UK) in fluorescence-activated cell sorting (FACS) buffer [phosphate-buffered saline (PBS) containing 2% heat-inactivated foetal calf serum (FCS; Invitrogen) and 5 mM ethylenediaminetetraacetic acid (EDTA; Invitrogen)]. Erythrocytes from

splenic samples were osmotically lysed in ACK lysis buffer (Invitrogen) and cells washed twice in FACS buffer.

Cell culture

OP9-DL1 cells (kindly provided by J.C Zúniga-Pflücker, Sunnybrook Research Institute, Toronto) [27] were maintained at 75% confluency in Dulbecco's modified Eagles' medium (DMEM) with GlutaMAX (Invitrogen), 10% FCS, 1% penicillin and streptomycin, 50 μM β-mercaptoethanol (Invitrogen), and 1% non-essential amino acids (Invitrogen) at 37°C and 5% CO_2. Foetal thymocytes from WT or *p110δ*$^{-/-}$ E15 thymic lobes were isolated and seeded onto a semi-confluent monolayer of OP9-DL1 cells cultured in flat-bottom 96-well plates with 200 μl of complete DMEM medium supplemented with 5 ng/ml Flt3 ligand (Miltenyi Biotec) and 1 ng/ml IL-7 (Miltenyi Biotec). IL-7 and Flt3 ligand were replenished every 3 days. Cells were cultured for 8 days at 37°C and 5% CO_2, followed by analysis by flow cytometry.

Flow cytometry

Fluorochrome-conjugated antibodies (purchased from eBioscience, BD, Biolegend or Cell Signaling Technology, unless otherwise indicated) against the following cell surface and intracellular molecules were used: rabbit Ig Alexa-488, rabbit Ig Alexa-647, rat IgM (RM-7B4), Annexin V, Blk, CD3ε (145-2C11), CD8α (53-6.7), CD8β (H35-17.2), CD24 (M1/69), CD44 (IM7), CD45RB (C363.16A), CD121a (IL-1Rα; JAMA-147), CD127 (IL-7Rα; SB/199), c-Maf (sym0F1), Foxo1 (C29H4), IFNγ (XMG1.2), IL-17A (eBio17B7), Lck (73A5), Ly6A/E (Sca-1; D7), pAkt (Ser473; D9E), pSyk (pY348; I120-722), pS6 (Ser235/236; D57.2.2E), RORγt (B2D), TCRδ (GL3), Vγ1 (2.11), Vγ4 (UC3-10A6), Vγ5 (536), Vγ7 (F2.67; kindly provided by Dr Pablo Pereira, Pasteur Institute, Paris), Syk (5F5), Zap70 (1E7.2), and 17D1 (kindly provided by Prof Adrian Hayday, Francis Crick Institute, London). For cell surface staining, thymocytes and lymphocytes were incubated on ice with CD16/CD32-specific antibodies (2.4G2; eBioscience) to block Fc receptors and stained with fluorochrome-conjugated antibodies diluted in FACS buffer. Detection of both Vγ5Vδ1 and Vγ6Vδ1 with 17D1 was performed as previously described [20]. After staining, cells were washed and re-suspended in FACS buffer. 4',6-diamidino-2-phenylindole (DAPI; Invitrogen), DRAQ7™ (Biolegend) or Zombie Aqua™ Fixable Viability dye (Biolegend) were used for dead cell exclusion prior to analysis. For detection of intracellular molecules, cells were stained for surface markers and Zombie Aqua™ Fixable Viability dye (Biolegend) for dead cell exclusion, fixed with IC fixation buffer (eBioscience) for 15 min on ice

and subsequently permeabilized and stained with intracellular antibodies diluted in permeabilization buffer (eBioscience). For intracellular cytokine staining, cells were stimulated, prior to staining, with 50 ng/ml phorbol 12-myristate 13-acetate (PMA; Sigma) and 1 μg/ml ionomycin (Sigma) for 4h at 37°C; 10 μg/ml Brefeldin A (eBioscience) and 2μM Monensin (eBioscience) were added during the last 2 h. For intracellular detection of pAkt, pSyk, or pS6, thymic lobes were collected directly in chilled tubes containing fluorochrome-conjugated antibody staining mix and immediately homogenised to release thymocytes. After a 10-min incubation on ice for cell surface marker staining, cells were fixed with IC fixation buffer for 15 min on ice. For intracellular detection of transcription factors or Ki67, cells were fixed and permeabilised with the Foxp3/Transcription Factor buffer set (eBioscience) as per the manufacturer's instructions and subsequently stained with fluorochrome-conjugated antibodies. Samples were acquired using an LSR-II flow cytometer (BD) or Canto II (BD) and data were analysed using FlowJo software (Tree Star, Inc.).

Imagestream analysis

Thymic γδ T cells from 7-day FTOC were enriched by depleting $CD4^+$ cells using magnetic-activated cell sorting (MACS), according to the manufacturer's instructions (Miltenyi Biotec). Briefly, cells were surface stained with biotin-conjugated anti-CD4 antibody (RM4.4; eBioscience) and subsequently labelled with anti-biotin microbeads (Miltenyi Biotec). Labelled cells were magnetically sorted and the flow-through was retained for cell surface and intracellular staining. Cells were resuspended in FACS buffer and nuclei were stained with DAPI just prior to sample acquisition using the Imagestream multispectral imaging flow cytometer (Amnis). Corresponding images were analysed using the IDEAS software after single in-focus cells were selected based on a gating strategy using gradient RMS and area versus aspect ratio.

Cell sorting and generation of single cell RNA-seq libraries

Thymocytes from WT E15 thymic lobes cultured for 8 days in the presence or absence of pan-PI3K inhibitor ZSTK474 (0.25 μM) were isolated and stained for cell surface molecules as described above, and total γδ T cells were sorted on a FACSAria (BD). Sorted cells were depleted of non-viable cells by low density gradient centrifugation. Viable cells were collected, counted and diluted to 1000 cells/μl. Single cell sequencing libraries were generated using the Chromium™ Single Cell 5' Library and Gel Bead Kit (10X Genomics) according to the manufacturer's instructions. Briefly, following the capture and lysis of single cells, cDNA was

synthesised, amplified and uniquely indexed libraries were pooled for sequencing (Illumina NextSeq).

Analysis of single-cell RNA-seq data

Analyses of RNA-seq data was carried out in R v3 using the package Seurat v2.3 [56]. Quality control measures were undertaken to obtain high-quality data for further analysis by filtering out cells with a gene number less than 200 or more than 3000, cells with more than 20% mitochondrial genes, and genes expressed in less than 3 cells. Datasets from control and pan-PI3K inhibitor-treated samples were integrated for comparative analyses. Subsequently, highly variable genes were defined and scaled data was subjected to principal component analysis. Statistically significant principle components (PCs) were identified based on the JackStraw method and Elbow plot method implemented in Seurat. Unsupervised graph-based clustering was performed using significant PCs and clustering resolution of 0.8, and visualised using the non-linear dimensional reduction technique, t-distributed Stochastic Neighbor Embedding (tSNE). After clustering, differentially expressed genes defining each cluster as well as between samples within a single cluster were identified. Gene ontology and enrichment pathway analysis was performed using Metascape [33].

Statistical analysis

Statistical analysis was performed using GraphPad Prism software. Data are presented as mean ± s.d. Student's *t*-test or one-way analysis of variance (ANOVA) were used to assess statistical significance of differences between groups. A difference was considered significant if $P \leq 0.05$.

SUPPLEMENTARY MATERIALS

Figs. S1 to S10

REFERENCES AND NOTES

1. Pauza, C.D., et al., *Targeting gammadelta T cells for immunotherapy of HIV disease.* Future Virol, 2011. **6**(1): p. 73-84.
2. Jameson, J.M., et al., *A role for the mevalonate pathway in the induction of subtype cross-reactive immunity to influenza A virus by human gammadelta T lymphocytes.* Cell Immunol, 2010. **264**(1): p. 71-7.
3. Behr, C., et al., *Plasmodium falciparum stimuli for human gammadelta T cells are related to phosphorylated antigens of mycobacteria.* Infect Immun, 1996. **64**(8): p. 2892-6.
4. Kabelitz, D., et al., *The primary response of human gamma/delta + T cells to Mycobacterium tuberculosis is restricted to V gamma 9-bearing cells.* J Exp Med, 1991. **173**(6): p. 1331-8.
5. Laggner, U., et al., *Identification of a novel proinflammatory human skin-homing Vgamma9Vdelta2 T cell subset with a potential role in psoriasis.* J Immunol, 2011. **187**(5): p. 2783-93.
6. Halder, R.C., et al., *Mini review: immune response to myelin-derived sulfatide and CNS-demyelination.* Neurochem Res, 2007. **32**(2): p. 257-62.
7. Gentles, A.J., et al., *The prognostic landscape of genes and infiltrating immune cells across human cancers.* Nat Med, 2015. **21**(8): p. 938-45.
8. Gao, Y., et al., *Gamma delta T cells provide an early source of interferon gamma in tumor immunity.* J Exp Med, 2003. **198**(3): p. 433-42.
9. Hamada, S., et al., *IL-17A produced by gamma delta T cells plays a critical role in innate immunity against Listeria monocytogenes infection in the liver.* Journal of Immunology, 2008. **181**(5): p. 3456-3463.
10. Dejima, T., et al., *Protective Role of Naturally Occurring Interleukin-17A-Producing gamma delta T Cells in the Lung at the Early Stage of Systemic Candidiasis in Mice.* Infection and Immunity, 2011. **79**(11): p. 4503-4510.
11. Prinz, I., B. Silva-Santos, and D.J. Pennington, *Functional development of gammadelta T cells.* Eur J Immunol, 2013. **43**(8): p. 1988-94.
12. Sumaria, N., S. Martin, and D.J. Pennington, *Developmental origins of murine gammadelta T-cell subsets.* Immunology, 2019. **156**(4): p. 299-304.
13. Haks, M.C., et al., *Attenuation of gammadeltaTCR signaling efficiently diverts thymocytes to the alphabeta lineage.* Immunity, 2005. **22**(5): p. 595-606.
14. Hayes, S.M., L. Li, and P.E. Love, *TCR signal strength influences alphabeta/gammadelta lineage fate.* Immunity, 2005. **22**(5): p. 583-93.

15. Kreslavsky, T., et al., *T cell receptor-instructed alphabeta versus gammadelta lineage commitment revealed by single-cell analysis.* J Exp Med, 2008. **205**(5): p. 1173-86.
16. Jensen, K.D., et al., *Thymic selection determines gammadelta T cell effector fate: antigen-naive cells make interleukin-17 and antigen-experienced cells make interferon gamma.* Immunity, 2008. **29**(1): p. 90-100.
17. Ribot, J.C., et al., *CD27 is a thymic determinant of the balance between interferon-gamma- and interleukin 17-producing gammadelta T cell subsets.* Nat Immunol, 2009. **10**(4): p. 427-36.
18. Turchinovich, G. and A.C. Hayday, *Skint-1 identifies a common molecular mechanism for the development of interferon-gamma-secreting versus interleukin-17-secreting gammadelta T cells.* Immunity, 2011. **35**(1): p. 59-68.
19. Munoz-Ruiz, M., et al., *TCR signal strength controls thymic differentiation of discrete proinflammatory gammadelta T cell subsets.* Nat Immunol, 2016. **17**(6): p. 721-727.
20. Sumaria, N., et al., *Strong TCRgammadelta Signaling Prohibits Thymic Development of IL-17A-Secreting gammadelta T Cells.* Cell Rep, 2017. **19**(12): p. 2469-2476.
21. Fahl, S.P., et al., *Role of a selecting ligand in shaping the murine gammadelta-TCR repertoire.* Proc Natl Acad Sci U S A, 2018. **115**(8): p. 1889-1894.
22. Lopes, N., et al., *Distinct metabolic programs established in the thymus control effector functions of gammadelta T cell subsets in tumor microenvironments.* Nat Immunol, 2021. **22**(2): p. 179-192.
23. Jenkinson, E.J., G. Anderson, and J.J. Owen, *Studies on T cell maturation on defined thymic stromal cell populations in vitro.* J Exp Med, 1992. **176**(3): p. 845-53.
24. Chu, D.H., et al., *Pre-T cell receptor signals are responsible for the down-regulation of Syk protein tyrosine kinase expression.* J Immunol, 1999. **163**(5): p. 2610-20.
25. Yamamoto, N., et al., *The orally available spleen tyrosine kinase inhibitor 2-[7-(3,4-dimethoxyphenyl)-imidazo[1,2-c]pyrimidin-5-ylamino]nicotinamide dihydrochloride (BAY 61-3606) blocks antigen-induced airway inflammation in rodents.* J Pharmacol Exp Ther, 2003. **306**(3): p. 1174-81.
26. Roller, A., et al., *Blockade of phosphatidylinositol 3-kinase (PI3K)delta or PI3Kgamma reduces IL-17 and ameliorates imiquimod-induced psoriasis-like dermatitis.* J Immunol, 2012. **189**(9): p. 4612-20.
27. de Pooter, R. and J.C. Zuniga-Pflucker, *T-cell potential and development in vitro: the OP9-DL1 approach.* Curr Opin Immunol, 2007. **19**(2): p. 163-8.

28. Okkenhaug, K., K. Ali, and B. Vanhaesebroeck, *Antigen receptor signalling: a distinctive role for the p110delta isoform of PI3K.* Trends Immunol, 2007. **28**(2): p. 80-7.
29. Stark, A.K., et al., *PI3Kdelta hyper-activation promotes development of B cells that exacerbate Streptococcus pneumoniae infection in an antibody-independent manner.* Nat Commun, 2018. **9**(1): p. 3174.
30. Barata, J.T., et al., *Activation of PI3K is indispensable for interleukin 7-mediated viability, proliferation, glucose use, and growth of T cell acute lymphoblastic leukemia cells.* J Exp Med, 2004. **200**(5): p. 659-69.
31. Michel, M.L., et al., *Interleukin 7 (IL-7) selectively promotes mouse and human IL-17-producing gammadelta cells.* Proc Natl Acad Sci U S A, 2012. **109**(43): p. 17549-54.
32. Tan, L., et al., *Single-Cell Transcriptomics Identifies the Adaptation of Scart1(+) Vgamma6(+) T Cells to Skin Residency as Activated Effector Cells.* Cell Rep, 2019. **27**(12): p. 3657-3671 e4.
33. Zhou, Y., et al., *Metascape provides a biologist-oriented resource for the analysis of systems-level datasets.* Nat Commun, 2019. **10**(1): p. 1523.
34. Martinet, V., et al., *Type I interferons regulate eomesodermin expression and the development of unconventional memory CD8(+) T cells.* Nat Commun, 2015. **6**: p. 7089.
35. Hedrick, S.M., et al., *FOXO transcription factors throughout T cell biology.* Nat Rev Immunol, 2012. **12**(9): p. 649-61.
36. Zuberbuehler, M.K., et al., *The transcription factor c-Maf is essential for the commitment of IL-17-producing gammadelta T cells.* Nat Immunol, 2019. **20**(1): p. 73-85.
37. Muro, R., et al., *gammadeltaTCR recruits the Syk/PI3K axis to drive proinflammatory differentiation program.* J Clin Invest, 2018. **128**(1): p. 415-426.
38. Zarin, P., et al., *Integration of T-cell receptor, Notch and cytokine signals programs mouse gammadelta T-cell effector differentiation.* Immunol Cell Biol, 2018. **96**(9): p. 994-1007.
39. Haas, J.D., et al., *Development of interleukin-17-producing gammadelta T cells is restricted to a functional embryonic wave.* Immunity, 2012. **37**(1): p. 48-59.
40. Kisielow, J., M. Kopf, and K. Karjalainen, *SCART scavenger receptors identify a novel subset of adult gammadelta T cells.* J Immunol, 2008. **181**(3): p. 1710-6.
41. Baldwin, C.L. and J.C. Telfer, *The bovine model for elucidating the role of gammadelta T cells in controlling infectious diseases of importance to cattle and humans.* Mol Immunol, 2015. **66**(1): p. 35-47.
42. Buus, T.B., et al., *Three distinct developmental pathways for adaptive and two IFN-gamma-producing gammadelta T subsets in adult thymus.* Nat Commun, 2017. **8**(1): p. 1911.

43. van de Pavert, S.A. and E. Vivier, *Differentiation and function of group 3 innate lymphoid cells, from embryo to adult.* Int Immunol, 2016. **28**(1): p. 35-42.
44. Zhong, C., M. Zheng, and J. Zhu, *Lymphoid tissue inducer-A divergent member of the ILC family.* Cytokine Growth Factor Rev, 2018. **42**: p. 5-12.
45. Shibata, K., et al., *IFN-gamma-producing and IL-17-producing gammadelta T cells differentiate at distinct developmental stages in murine fetal thymus.* J Immunol, 2014. **192**(5): p. 2210-8.
46. Malhotra, N., et al., *A network of high-mobility group box transcription factors programs innate interleukin-17 production.* Immunity, 2013. **38**(4): p. 681-93.
47. Gray, E.E., et al., *Deficiency in IL-17-committed Vgamma4(+) gammadelta T cells in a spontaneous Sox13-mutant CD45.1(+) congenic mouse substrain provides protection from dermatitis.* Nat Immunol, 2013. **14**(6): p. 584-92.
48. Spidale, N.A., et al., *Interleukin-17-Producing gammadelta T Cells Originate from SOX13(+) Progenitors that Are Independent of gammadeltaTCR Signaling.* Immunity, 2018. **49**(5): p. 857-872 e5.
49. Lienenklaus, S., et al., *Novel reporter mouse reveals constitutive and inflammatory expression of IFN-beta in vivo.* J Immunol, 2009. **183**(5): p. 3229-36.
50. Xing, Y., et al., *Late stages of T cell maturation in the thymus involve NF-kappaB and tonic type I interferon signaling.* Nat Immunol, 2016. **17**(5): p. 565-73.
51. Henry, T., et al., *Type I IFN signaling constrains IL-17A/F secretion by gammadelta T cells during bacterial infections.* J Immunol, 2010. **184**(7): p. 3755-67.
52. Li, W., B. Moltedo, and T.M. Moran, *Type I interferon induction during influenza virus infection increases susceptibility to secondary Streptococcus pneumoniae infection by negative regulation of gammadelta T cells.* J Virol, 2012. **86**(22): p. 12304-12.
53. Mayer-Barber, K.D. and B. Yan, *Clash of the Cytokine Titans: counter-regulation of interleukin-1 and type I interferon-mediated inflammatory responses.* Cell Mol Immunol, 2017. **14**(1): p. 22-35.
54. Okkenhaug, K., et al., *Impaired B and T cell antigen receptor signaling in p110delta PI 3-kinase mutant mice.* Science, 2002. **297**(5583): p. 1031-4.
55. Lochner, M., et al., *In vivo equilibrium of proinflammatory IL-17+ and regulatory IL-10+ Foxp3+ RORgamma t+ T cells.* J Exp Med, 2008. **205**(6): p. 1381-93.
56. Butler, A., et al., *Integrating single-cell transcriptomic data across different conditions, technologies, and species.* Nat Biotechnol, 2018. **36**(5): p. 411-420.

Acknowledgements: We thank our BSU, flow facilities and the Genome Centre for technical assistance. **Funding:** This work was supported by grants from the Wellcome Trust (092973/Z/10/Z) and BBSRC (BB/R017808/1). **Author contributions:** N.S. performed experiments with assistance from S.M.. D.J.P. and N.S. designed the study, analysed the data, and wrote the manuscript. **Competing interests:** The authors declare that they have no competing interests. **Data and materials availability:** The single-cell RNA sequencing data have been deposited in the GEO public repository (https://www.ncbi.nlm.nih.gov/geo/) with the accession code GSE167943. All other data needed to evaluate the conclusions in the paper are present in the paper or the Supplementary Materials.

FIGURE LEGENDS

Fig. 1. Development of $\gamma\delta^{17}$ cells requires constrained Syk activity. (**A**) Flow cytometry plots of $\gamma\delta$ T cells from WT E15 thymic lobes after 7-day FTOC showing total TCRδ^+ cells ($\gamma\delta^+$ cells) and CD24$^-$ $\gamma\delta$ ($\gamma\delta^{24-}$) T cells. Histograms show the abundance of Lck, Zap70, and Syk in the indicated $\gamma\delta$ T cell subsets. Summary graphs show mean fluorescence intensity (MFI) of Lck, Zap70, and Syk in the indicated $\gamma\delta$ T cell subsets. Data are representative of at least two independent experiments. Each symbol represents at least 4 thymic lobes pooled. (**B**) Histogram shows the abundance of phosphorylated Syk (pSyk) in CD24$^+$ $\gamma\delta$ ($\gamma\delta^{24+}$) T cells from WT neonatal thymocytes treated with the indicated concentrations of the Syk inhibitor BAY-61-3606 (BAY-61) or left untreated for 2h. Percentages of pSyk-positive cells are indicated. Summary graph shows the relative MFI of intracellular pSyk (*n* = 3 replicates per group, where each replicate represents 2 neonatal thymuses pooled). (**C**) Plots show $\gamma\delta^{24-}$ T cells from WT E15 7-day FTOC in the absence or presence of the indicated concentrations of BAY-61-3606. Data are representative of two independent experiments. (**D**) Plots show $\gamma\delta^{24-}$ T cells from WT E15 7-day FTOC in the absence or presence of the TCRδ-activating antibody GL3 (concentrations indicated) and BAY-61-3606 (0.4 μM). Summary graph shows absolute number of $\gamma\delta^{17}$ cells in each condition. Each symbol represents at least 2 thymic lobes pooled. Percentages of gated cells are indicated in plots. Error bars represent s.d. TN, triple negative for CD24, CD44 and CD45RB; RB, CD45RB$^+$. *$P \leq 0.05$, **$P \leq 0.01$ and ***$P \leq 0.001$ (ANOVA with Dunnett's test).

Fig. 2. Generation of $\gamma\delta^{17}$ cells requires PI3K activity. (**A**) Flow plots show $\gamma\delta^{24-}$ T cells from lymph nodes (LN) of WT and *p110δ*$^{-/-}$ mice to quantify $\gamma\delta^{17}$ ($CD24^{-}CD45RB^{-}CD44^{+}$) cells. The $\gamma\delta^{17}$ cells were stimulated ex vivo with the T cell activators PMA and ionomycin for 4h before measuring IL-17 and IFNγ. Summary graph shows absolute numbers of IL-17^{+} $\gamma\delta^{17}$ cells. Data are representative of three independent experiments ($n \geq 5$ mice per group). (**B**) Plots show $\gamma\delta^{24-}$ T cells from 7-day FTOC of E15 thymic lobes from WT or *p110δ*$^{-/-}$ mice and IL-17 and IFNγ in $\gamma\delta^{17}$ cells after 3h PMA and ionomycin stimulation. Summary graphs show absolute number of $\gamma\delta^{17}$ cells and IL-17^{+} $\gamma\delta^{17}$ cells. Data are representative of six independent experiments. (**C**) Plots show $\gamma\delta^{24-}$ T cells from 14-day FTOC of WT or *p110δ*$^{-/-}$ E15 thymic lobes. Pie charts depict Vγ-usage by $\gamma\delta^{17}$ cells from the same cultures. Data are representative of two independent experiments. (**D**) Plots show $\gamma\delta^{24-}$ T cells from 8-day co-culture of thymocytes isolated from WT or *p110δ*$^{-/-}$ E15 thymic lobes with OP9-DL1 stromal cells. IL-17 and IFNγ was measured in $\gamma\delta^{17}$ cells from these cultures after 3h PMA and ionomycin stimulation. Summary graph shows percentage of $\gamma\delta^{17}$ cells from the cultures. Data are representative of two independent experiments. (**E** and **F**) Plots show $\gamma\delta^{24-}$ T cells from 7-day FTOC of WT E15 thymic lobes in the presence or absence of the pan-Akt inhibitor MK-2206 (0.125 μM) (E) or the PTEN inhibitor SF1670 (2 μM) (F). (**G**) Plots show $\gamma\delta^{24-}$ T cells from 7-day FTOC of $p110\delta^{WT}$ or $p110\delta^{E1020K}$ E15 thymic lobes. Summary graphs show absolute number of $\gamma\delta^{17}$ cells in the cultures. Data are representative of two (E and G) or five (F) independent experiments. (**H**) Plots show $\gamma\delta^{24-}$ T cells from lymph nodes of adult $p110\delta^{WT}$ and $p110\delta^{E1020K}$ mice and IL-17 and IFNγ in $\gamma\delta^{17}$ cells after 4h PMA and ionomycin stimulation. Summary graph shows absolute number of IL-17^{+} $\gamma\delta^{17}$ cells. Data are representative of two independent experiments ($n = 5$ mice per group). Percentages of gated cells and γδ subset are indicated on plots. Each symbol represents an individual mouse or

at least four thymic lobes pooled. *$P \leq 0.05$, **$P \leq 0.01$ and ***$P \leq 0.001$ (Unpaired Student's *t*-test).

Fig. 3. Constrained TCRγδ-associated Syk activity stimulates the PI3K pathway to generate $\gamma\delta^{17}$ cells. (**A**) Graph shows relative mean fluorescence intensity (MFI) of intracellular phosphorylated Akt (pAkt) in γδ T cells from 1-day FTOC of WT E15 thymic lobes in the presence or absence of the pan-PI3K inhibitor ZSTK474 (pan-PI3K inh, 0.25 μM) or the Syk inhibitor BAY-61-3606 (Syk inh, 0.4 μM). Data are from three independent experiments (*n* = 10 replicates per group, where each replicate represents at least 3 thymic lobes pooled). (**B** to **D**) Plots of $\gamma\delta^{24-}$ T cells from 7-day FTOC of WT E15 thymic lobes in the presence or absence of GL3 (concentrations indicated) and/or the pan-PI3K inhibitor (0.25 μM) (B); in the presence of the indicated combinations of the Syk inhibitor (0.1 μM) and the PTEN inhibitor (2 μM) (C); and in the presence of the indicated combinations of GL3 (0.1 μg/ml), and the PTEN inhibitor (2 μM) (D). Data are representative of two independent experiments. (**E** and **F**) Graphs show relative MFI of intracellular pSyk (E) and phosphorylated S6 (pS6) (F) in $\gamma\delta^{24+}$ T cells from 4h FTOC of WT E15 thymic lobes in the presence or absence of GL3 (1 μg/ml) or the Syk inhibitor (0.4 μM) as indicated. Data are from one (E), or three (F) independent experiments (*n* = 3 to 8 replicates per group, where each replicate represents at least 2 thymic lobes pooled). (**G** and **H**) Plots of $\gamma\delta^{24-}$ T cells from 7-day FTOC of WT E15 thymic lobes in the indicated combinations of the pan-PI3K inhibitor (0.25 μM), the Syk inhibitor (0.4 μM), and the MEK inhibitor UO126 (5 μM) (G) or the indicated combinations of the Syk inhibitor (0.4 μM), IL-1β (5 ng/ml), and IL-7 (10 ng/ml) (H). Data are representative of two independent experiments. Summary graphs (C, D, G and H) show the absolute number of $\gamma\delta^{17}$ cells in the cultures. Each symbol represents at least four thymic lobes pooled. Percentages of gated cells and γδ subset are indicated on plots. Error bars represent s.d. $*P \leq 0.05$, $**P \leq 0.01$ and $***P \leq 0.001$ (Unpaired Student's *t*-test (E) or ANOVA with Dunnett's test (A, C, D, F to H)).

Fig. 4. PI3K inhibition reveals a previously undescribed γδ T cell–associated transcriptional program. (**A**) Flow plots show $\gamma\delta^{24-}$ T cells from 8-day FTOC of WT E15 thymic lobes in the presence or absence of the pan-PI3K inhibitor ZSTK474 (0.25 μM). The γδ T cells from these organ cultures were used for scRNA-seq, the results of which are illustrated in the t-SNE plot. Each dot represents a single cell. (**B**) t-SNE representations show expression of genes associated with the IL-17-secreting developmental program in control or PI3K-inhibited γδ T cells. (**C**) Heatmap shows differentially expressed genes (DEGs) in $\gamma\delta^{17}$ cells from control versus PI3K-inhibited FTOC (adjusted $P \leq 0.05$). (**D**) Heatmap illustrates the expression of the top 20 DEGs that increased within the indicated γδ subsets in control or PI3K-inhibited FTOC (adjusted $P \leq 0.05$). Each column is the expression profile of a single cell. (**E**) Metascape pathway analysis of DEGs that increased in $\gamma\delta^{17}$ cells from PI3K inhibitor–treated FTOC. Only the most enriched pathways are illustrated. (**F**) Large t-SNE representation shows γδ T cells from untreated 8-day FTOC of WT E15 thymic lobes. Each dot represents a single cell, and each cluster is coloured and numbered. Smaller plots show expression of *Cd8b1* and *Ly6a*. Demarcated clusters (dashed lines) correspond to a single or a group of γδ subsets as indicated, or the expression of *Cd8b1* and *Ly6a*. (**G**) Flow plots show γδ T cells from 7-day FTOC of WT E15 thymic lobes in the presence or absence of IFN-β (200 U/ml). Summary graph shows absolute number of $CD8\beta^{+}$ non-$\gamma\delta^{17}$ cells. Data are representative of two independent experiments. Each symbol represents at least 3 thymic lobes pooled. Percentages of gated cells and γδ subset are indicated on plots. *$P \leq 0.05$ (Unpaired Student's *t*-test).

Fig. 5. Impairment of Syk-PI3K signaling attenuates IL-17-program master-regulator genes in developing γδ progenitors. (**A** to **C**) Plots of γδ T cells from 6-day FTOC of E15 thymic lobes from mice expressing GFP (RORγt) in the absence or presence of the pan-PI3K inhibitor ZSTK474 (0.25 μM) (A), the Syk inhibitor BAY-61-3606 (0.4 μM) (B), or GL3 (1 μg/ml) (C). For each treatment, the $\gamma\delta^{24+/TN}$ subset of the total γδ T cell population was further analysed for GFP expression plotted against side-scatter (SSC). Summary graphs show the percentage GFP^+ cells in the $\gamma\delta^{24+/TN}$ population and the mean fluorescence intensity (MFI) in GFP^+ cells. (**D**) Plots of γδ T cells from 6-day FTOC of WT E15 thymic lobes in the absence or presence of the pan-PI3K inhibitor (0.25 μM), the Syk inhibitor (0.4 μM), or GL3 (1 μg/ml). The $\gamma\delta^{24+/TN}$ cells from the total γδ T cell population were further analysed for c-Maf. Summary graphs show the percentage of $c\text{-}Maf^+$ cells in the $\gamma\delta^{24+/TN}$ population and the MFI of c-Maf in those cells. Percentages of gated cells and γδ subset are indicated on plots. Data are representative of two independent experiments. Each symbol represents at least 4 thymic lobes pooled. $^*P \leq 0.05$, $^{**}P \leq 0.01$ and $^{***}P \leq 0.001$ (Unpaired Student's *t*-test (A to C) or ANOVA with Dunnett's test (D)).

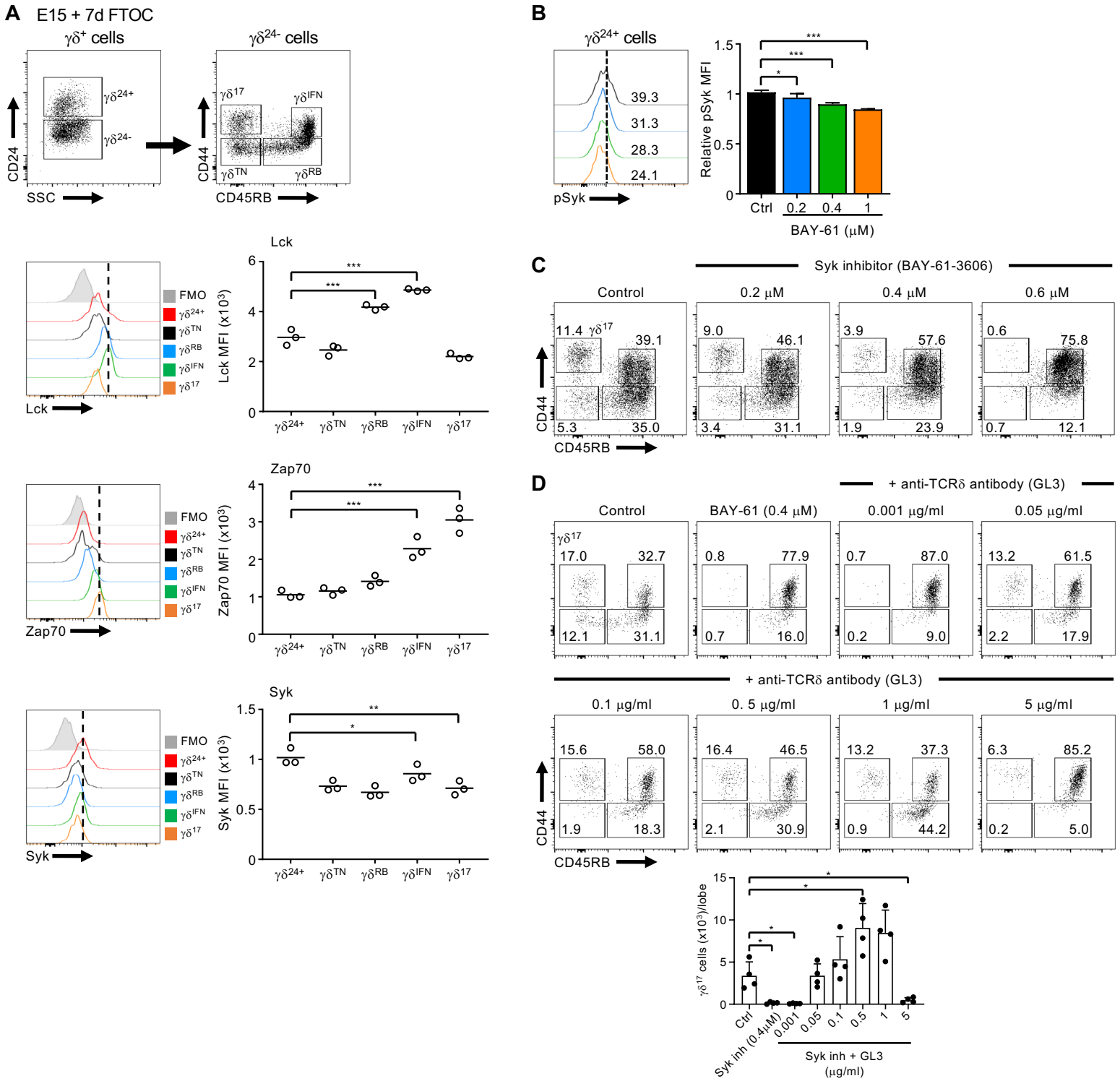
A
E15 + 7d FTOC
γδ+ cells
γδ24- cells
γδ24+
γδ24-
γδ17
γδIFN
γδTN
γδRB
CD24
SSC
CD44
CD45RB
Lck
Zap70
Syk
FMO
Lck MFI (x10³)
Zap70 MFI (x10³)
Syk MFI (x10³)
B
γδ24+ cells
39.3
31.3
28.3
24.1
pSyk
Relative pSyk MFI
Ctrl
0.2
0.4
1
BAY-61 (μM)
C
Syk inhibitor (BAY-61-3606)
Control
0.2 μM
0.4 μM
0.6 μM
11.4 γδ17
39.1
5.3
35.0
9.0
46.1
3.4
31.1
3.9
57.6
1.9
23.9
0.6
75.8
0.7
12.1
D
+ anti-TCRδ antibody (GL3)
Control
BAY-61 (0.4 μM)
0.001 μg/ml
0.05 μg/ml
γδ17
17.0
32.7
12.1
31.1
0.8
77.9
0.7
16.0
0.7
87.0
0.2
9.0
13.2
61.5
2.2
17.9
+ anti-TCRδ antibody (GL3)
0.1 μg/ml
0. 5 μg/ml
1 μg/ml
5 μg/ml
15.6
58.0
1.9
18.3
16.4
46.5
2.1
30.9
13.2
37.3
0.9
44.2
6.3
85.2
0.2
5.0
γδ17 cells (x10³)/lobe
Ctrl
Syk inh (0.4μM)
0.001
0.05
0.1
0.5
1
5
Syk inh + GL3
(μg/ml)

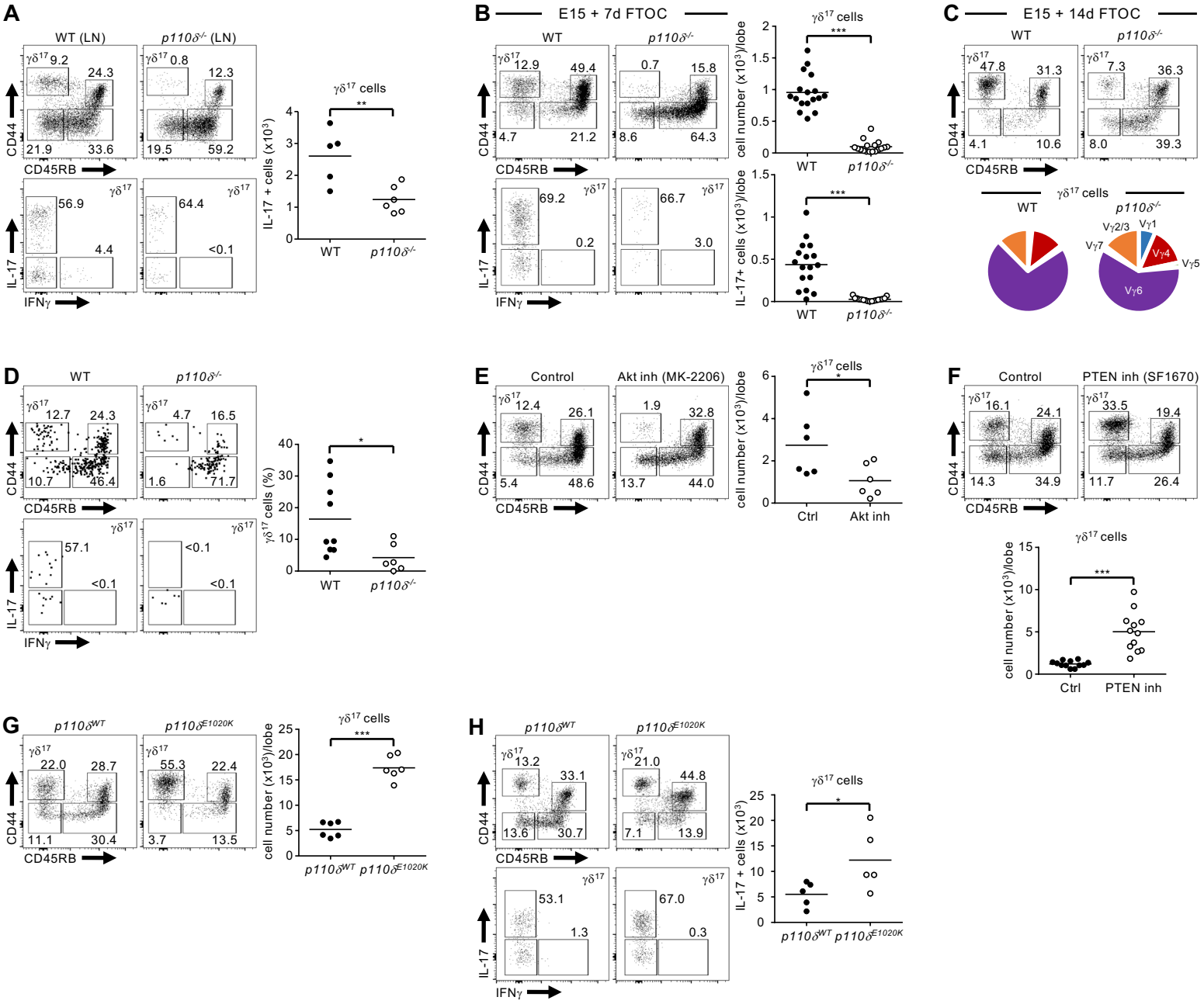
A
WT (LN)
p110δ-/- (LN)
γδ17 9.2
24.3
21.9
33.6
γδ17 0.8
12.3
19.5
59.2
CD44
CD45RB
γδ17
56.9
4.4
64.4
<0.1
IL-17
IFNγ
γδ17 cells
IL-17 + cells (x10³)
**
WT
p110δ-/-
B
E15 + 7d FTOC
WT
p110δ-/-
γδ17 12.9
49.4
4.7
21.2
0.7
15.8
8.6
64.3
69.2
0.2
66.7
3.0
γδ17 cells
cell number (x10³)/lobe
***
IL-17+ cells (x10³)/lobe
C
E15 + 14d FTOC
γδ17 47.8
31.3
4.1
10.6
7.3
36.3
8.0
39.3
γδ17 cells
Vγ2/3
Vγ1
Vγ7
Vγ4
Vγ5
Vγ6
D
γδ17 12.7
24.3
10.7
46.4
4.7
16.5
1.6
71.7
57.1
<0.1
γδ17 cells (%)
*
E
Control
Akt inh (MK-2206)
γδ17 12.4
26.1
5.4
48.6
1.9
32.8
13.7
44.0
Ctrl
Akt inh
F
Control
PTEN inh (SF1670)
γδ17 16.1
24.1
14.3
34.9
33.5
19.4
11.7
26.4
PTEN inh
G
p110δWT
p110δE1020K
γδ17 22.0
28.7
11.1
30.4
γδ17 55.3
22.4
3.7
13.5
H
γδ17 13.2
33.1
13.6
30.7
γδ17 21.0
44.8
7.1
13.9
53.1
1.3
67.0
0.3

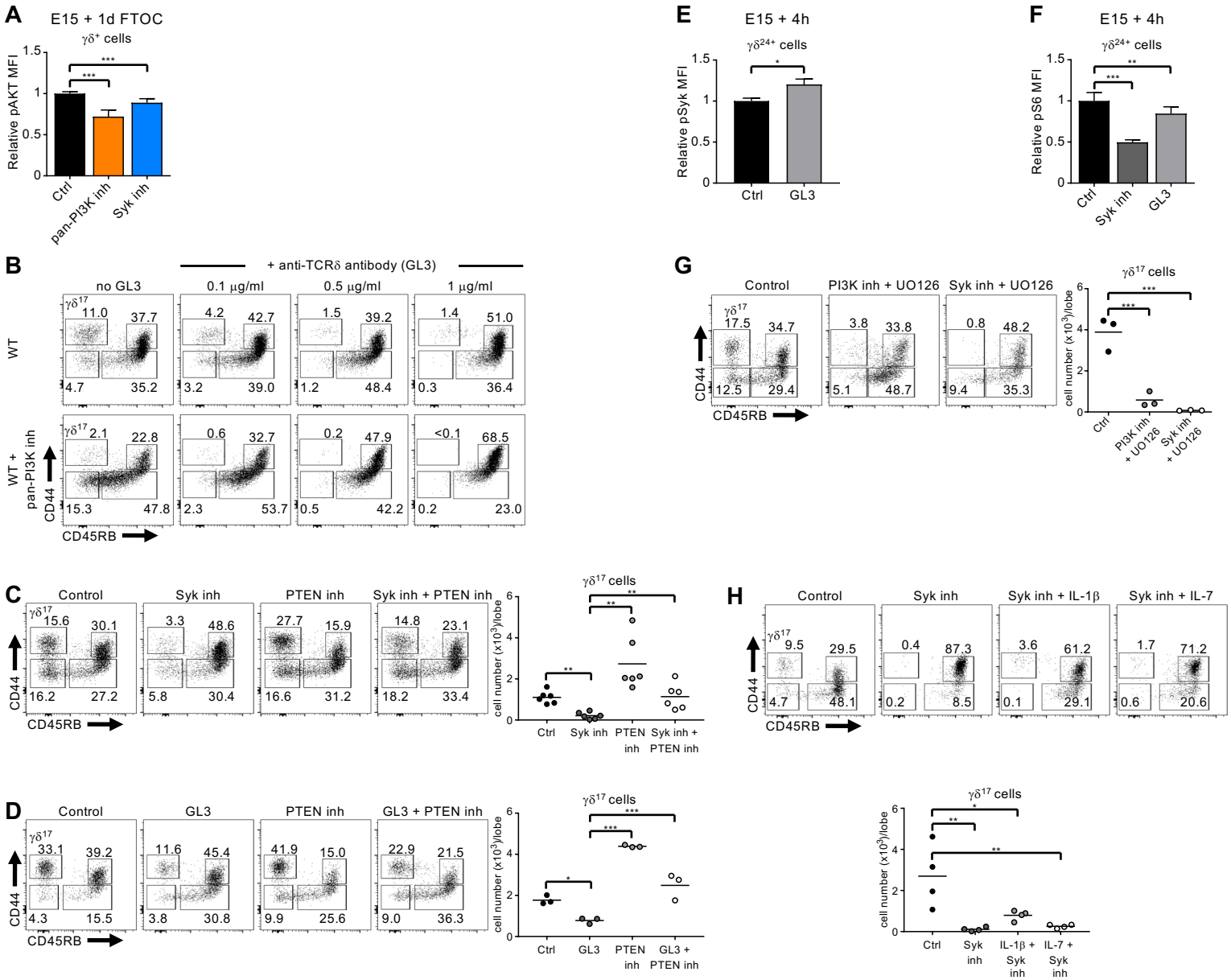
A
E15 + 1d FTOC
γδ+ cells
Relative pAKT MFI
Ctrl
pan-PI3K inh
Syk inh
B
+ anti-TCRδ antibody (GL3)
no GL3
0.1 μg/ml
0.5 μg/ml
1 μg/ml
WT
WT + pan-PI3K inh
CD44
CD45RB
C
Control
Syk inh
PTEN inh
Syk inh + PTEN inh
γδ17 cells
cell number (x10³)/lobe
D
Control
GL3
PTEN inh
GL3 + PTEN inh
E
E15 + 4h
γδ24+ cells
Relative pSyk MFI
Ctrl
GL3
F
E15 + 4h
γδ24+ cells
Relative pS6 MFI
Ctrl
Syk inh
GL3
G
Control
PI3K inh + UO126
Syk inh + UO126
γδ17 cells
cell number (x10³)/lobe
Ctrl
PI3K inh + UO126
Syk inh + UO126
H
Control
Syk inh
Syk inh + IL-1β
Syk inh + IL-7
γδ17 cells
cell number (x10³)/lobe
Ctrl
Syk inh
IL-1β + Syk inh
IL-7 + Syk inh

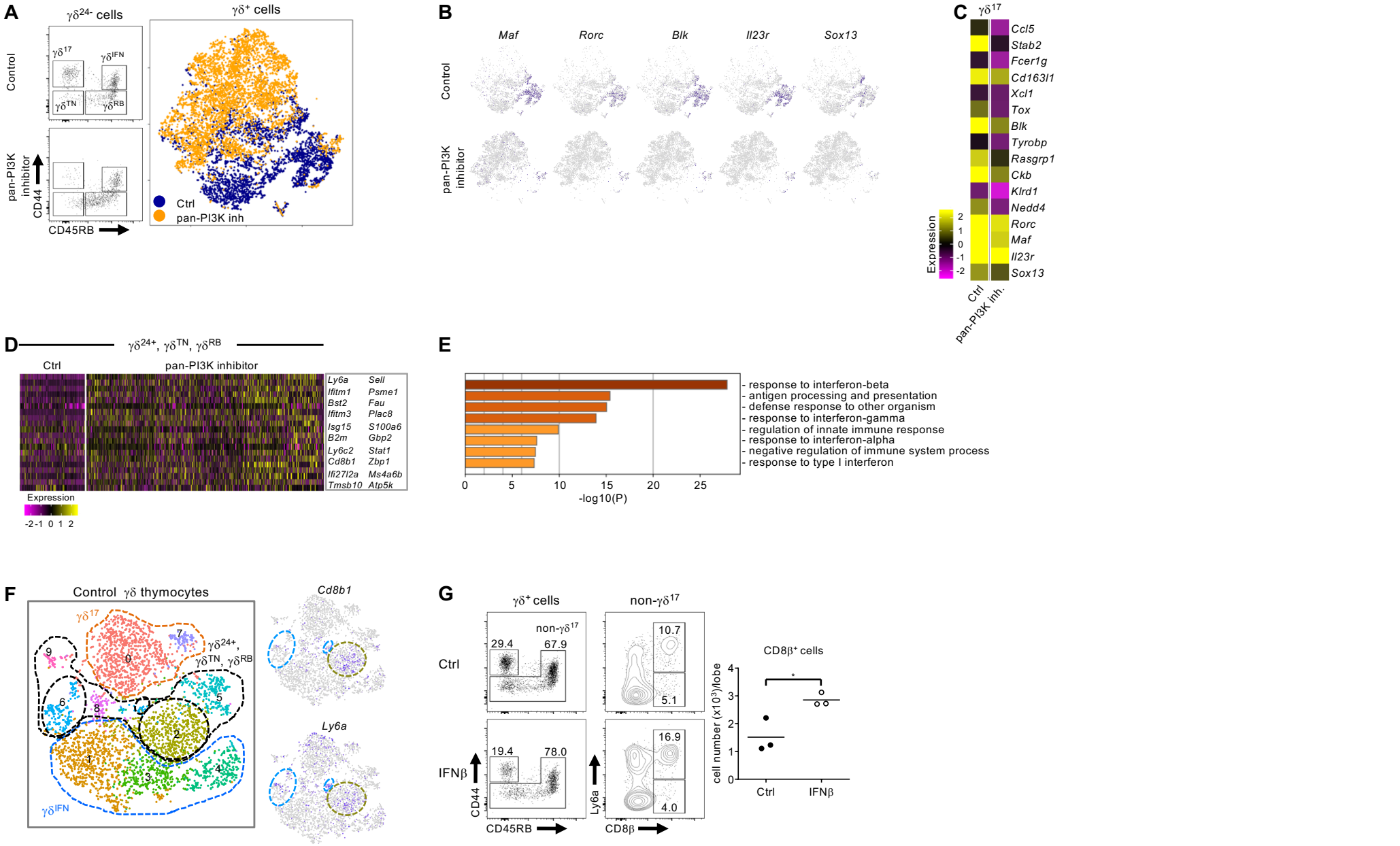
A
γδ24- cells
γδ+ cells
Control
pan-PI3K inhibitor
CD44
CD45RB
γδ17
γδIFN
γδTN
γδRB
Ctrl
pan-PI3K inh
B
Maf
Rorc
Blk
Il23r
Sox13
Control
pan-PI3K inhibitor
C
γδ17
Ccl5
Stab2
Fcer1g
Cd163l1
Xcl1
Tox
Blk
Tyrobp
Rasgrp1
Ckb
Klrd1
Nedd4
Rorc
Maf
Il23r
Sox13
Expression
2
1
0
-1
-2
Ctrl
pan-PI3K inh.
D
γδ24+, γδTN, γδRB
Ctrl
pan-PI3K inhibitor
Ly6a Sell
Ifitm1 Psme1
Bst2 Fau
Ifitm3 Plac8
Isg15 S100a6
B2m Gbp2
Ly6c2 Stat1
Cd8b1 Zbp1
Ifi27l2a Ms4a6b
Tmsb10 Atp5k
Expression
-2 -1 0 1 2
E
- response to interferon-beta
- antigen processing and presentation
- defense response to other organism
- response to interferon-gamma
- regulation of innate immune response
- response to interferon-alpha
- negative regulation of immune system process
- response to type I interferon
0
5
10
15
20
25
-log10(P)
F
Control γδ thymocytes
γδ17
γδIFN
γδ24+, γδTN, γδRB
0
1
2
3
4
5
6
7
8
9
Cd8b1
Ly6a
G
γδ+ cells
non-γδ17
Ctrl
IFNβ
29.4
67.9
10.7
5.1
19.4
78.0
16.9
4.0
CD44
CD45RB
Ly6a
CD8β
CD8β+ cells
cell number (x10³)/lobe
0
1
2
3
4
*
Ctrl
IFNβ

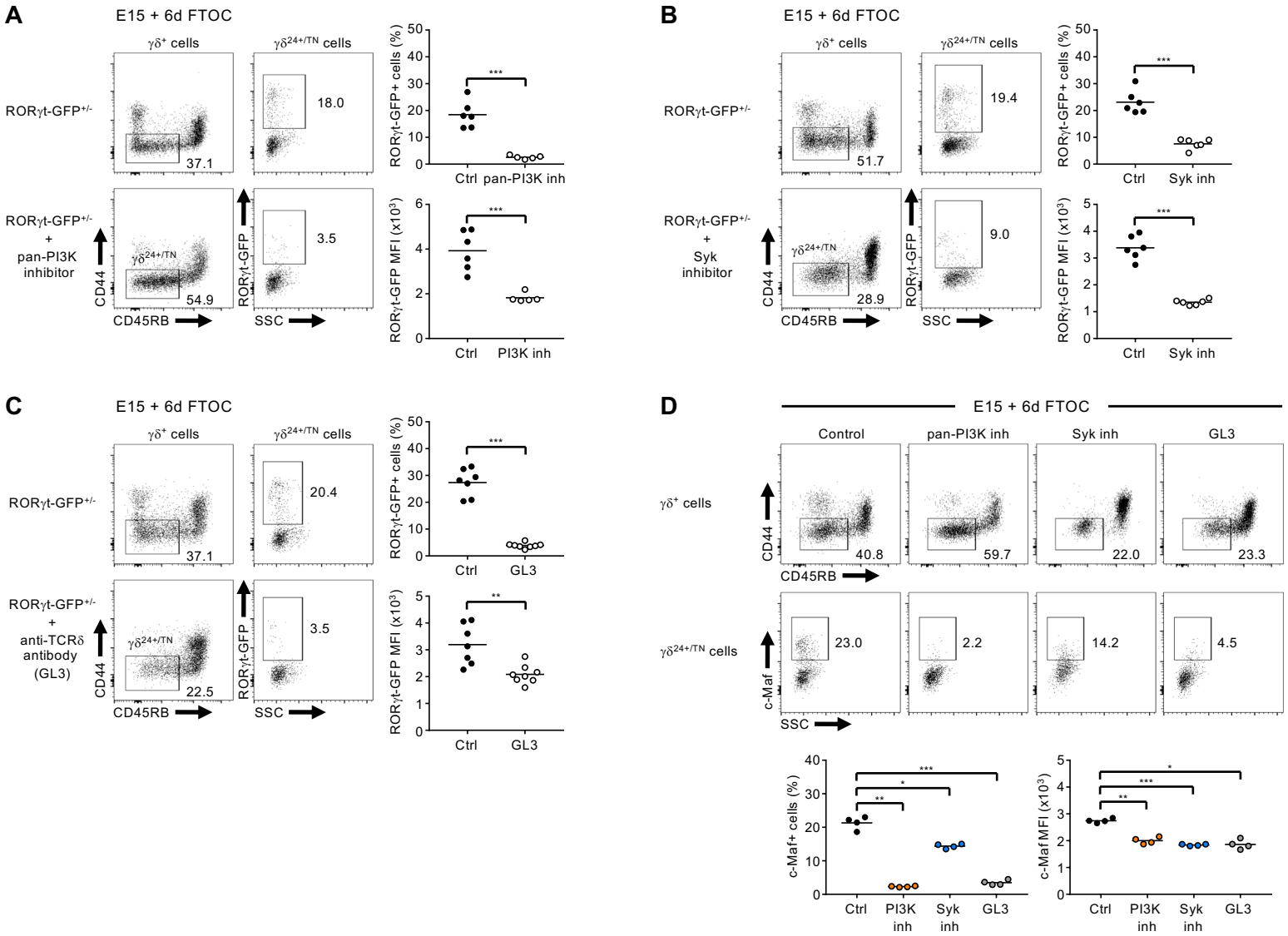
A
E15 + 6d FTOC
γδ+ cells
γδ24+/TN cells
RORγt-GFP+/-
RORγt-GFP+/-
+
pan-PI3K
inhibitor
37.1
18.0
54.9
3.5
CD44
CD45RB
RORγt-GFP
SSC
RORγt-GFP+ cells (%)
Ctrl
pan-PI3K inh
RORγt-GFP MFI (x10³)
PI3K inh
B
E15 + 6d FTOC
RORγt-GFP+/-
RORγt-GFP+/-
+
Syk
inhibitor
51.7
19.4
28.9
9.0
Syk inh
C
E15 + 6d FTOC
RORγt-GFP+/-
RORγt-GFP+/-
+
anti-TCRδ
antibody
(GL3)
37.1
20.4
22.5
3.5
GL3
D
E15 + 6d FTOC
Control
pan-PI3K inh
Syk inh
GL3
γδ+ cells
γδ24+/TN cells
40.8
59.7
22.0
23.3
23.0
2.2
14.2
4.5
c-Maf
SSC
c-Maf+ cells (%)
c-Maf MFI (x10³)
Ctrl
PI3K inh
Syk inh
GL3

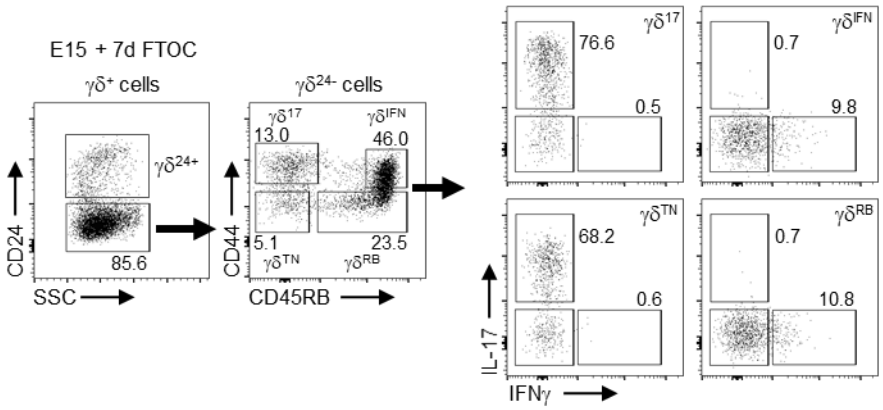

Fig. S1. CD24, CD44, and CD45RB segregate IL-17–producing and IFNγ–producing γδ T cells. Plots of γδ T cells from 7-day FTOC of WT E15 thymic lobes. $\gamma\delta^{24-}$ T cells from left panel are further sub-divided by CD44 and CD45RB (middle panel). Right panel shows intracellular staining for IL-17 and IFNγ in $\gamma\delta^{TN}$, $\gamma\delta^{RB}$, $\gamma\delta^{IFN}$ and $\gamma\delta^{17}$ subsets after 3h stimulation ex vivo with PMA and ionomycin. Data are representative of at least three independent experiments. TN is triple negative for CD24, CD44 and CD45RB; RB is CD45RB.

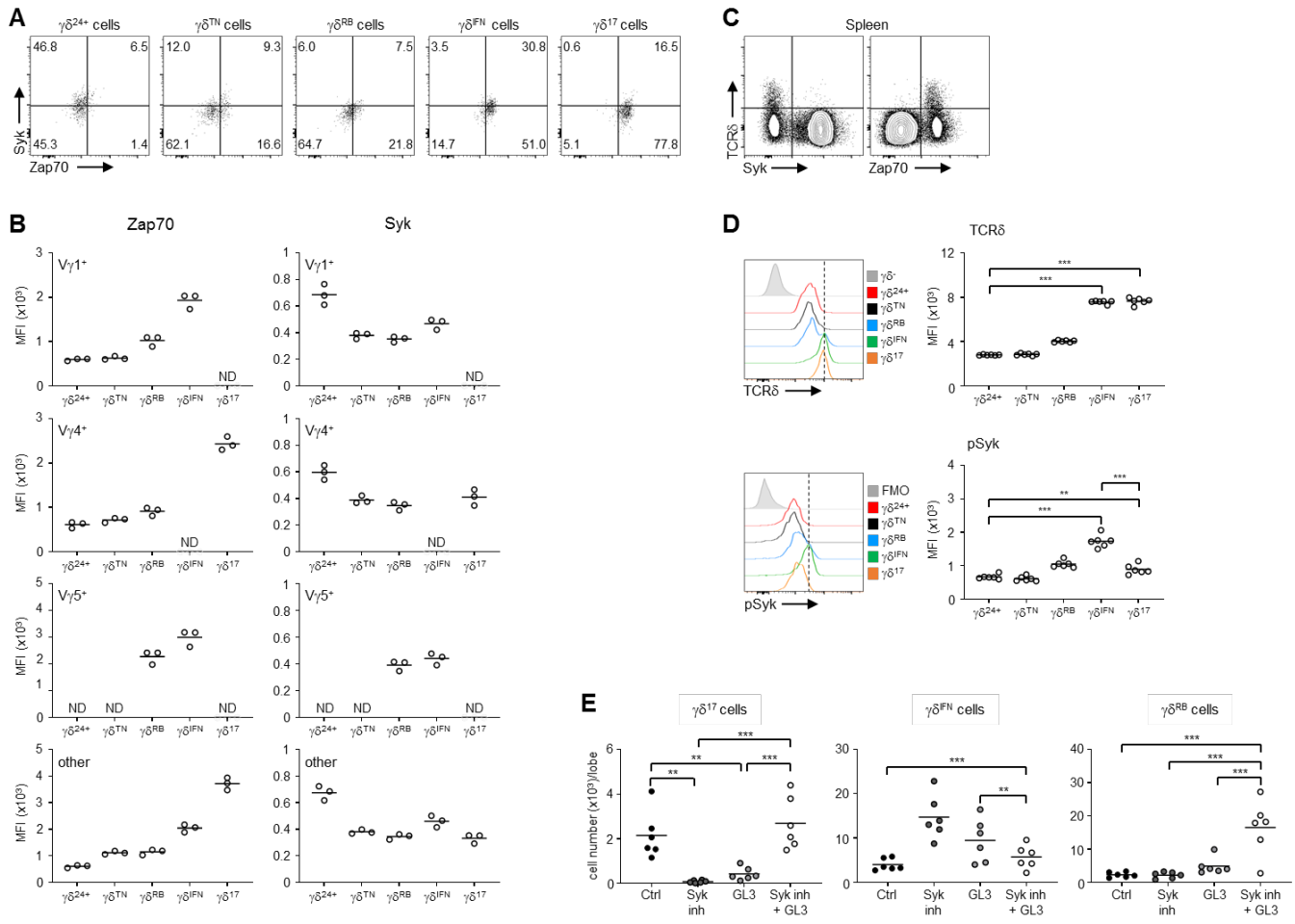

Fig. S2. Expression of Syk and Zap70 in thymic and peripheral γδ T cell subsets. (**A**) Plots show expression of Syk and Zap70 in indicated γδ T cell subsets from WT E15 thymic lobes after 7-day FTOC. Percentages of cells within each quadrant are indicated. Data are representative of three independent experiments. (**B**) Summary graphs show mean fluorescence intensity (MFI) of Zap70 and Syk in Vγ-specific γδ T cells, within indicated γδ T cell subsets, from WT E15 thymic lobes after 8-day FTOC. (**C**) Plots of splenic γδ T cells from adult WT mice showing intracellular expression of Syk or Zap70. Data are representative of two independent experiments. (**D**) Histograms show expression of TCRδ and pSyk in indicated γδ T cell subsets from WT E15 thymic lobes after 7-day FTOC. Summary graphs show MFI of TCRδ and pSyk in indicated γδ T cell subsets. (**E**) Summary graphs show absolute number of indicated γδ T cell subsets from WT E15 7-day FTOC in the presence (or absence) of Syk inhibitor BAY-61-3606 (0.4 μM), and/or anti-TCRδ antibody GL3 (1 μg/ml). Data are representative of two independent experiments. Each symbol represents at least 3 thymic lobes pooled. ND is no data. $^{**}P \leq 0.01$ and $^{***}P \leq 0.001$ (ANOVA with Dunnett's test).

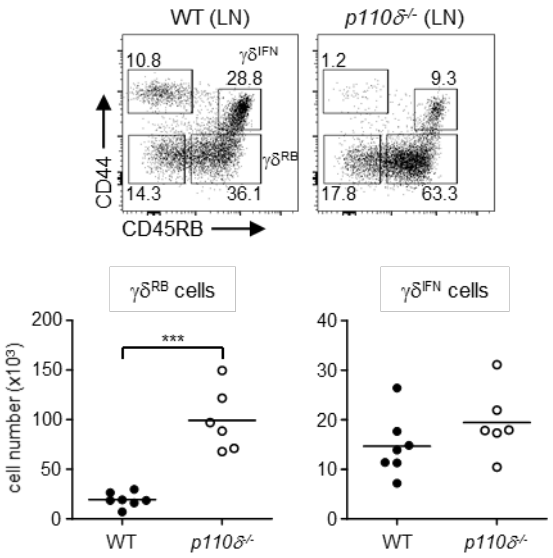

Fig. S3. γδ^{RB} cells expand in the absence of PI3K activity. Plots show γδ^{24-} T cells from WT and *p110δ*$^{-/-}$ adult lymph nodes (LN). Summary graphs show absolute number of γδ^{RB} and γδ^{IFN} cells. Data are representative of three independent experiments ($n \geq 5$ mice per group). ***$P \leq$ 0.001 (Unpaired Student's *t*-test).

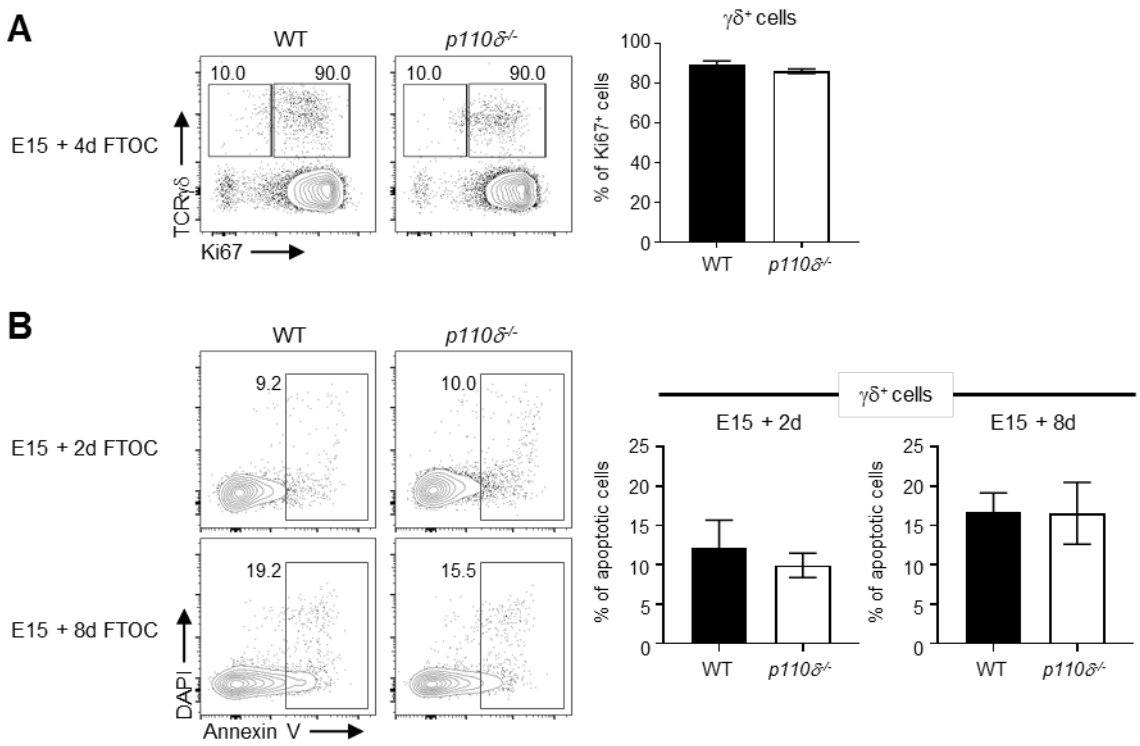

Fig. S4. Proliferation and apoptosis of thymic γδ T cells in PI3Kδ-deficient mice. (**A**) Plots show thymocytes from 4-day FTOC of WT or *p110δ*$^{-/-}$ E15 thymic lobes. Percentages of gated cells are indicated on plots. Summary graph shows percentage of Ki67^{+} γδ T cells (n = 3 replicates per group, where each replicate represents 2 thymic lobes pooled). (**B**) Plots show γδ T cells from 2-day FTOC of WT or *p110δ*$^{-/-}$ E15 thymic lobes. Percentages of gated cells are indicated on plots. Summary graph shows percentage of apoptotic (Annexin V^{+}) γδ T cells (n = 3 replicates per group, where each replicate represents 2 thymic lobes pooled). Error bars represent s.d.

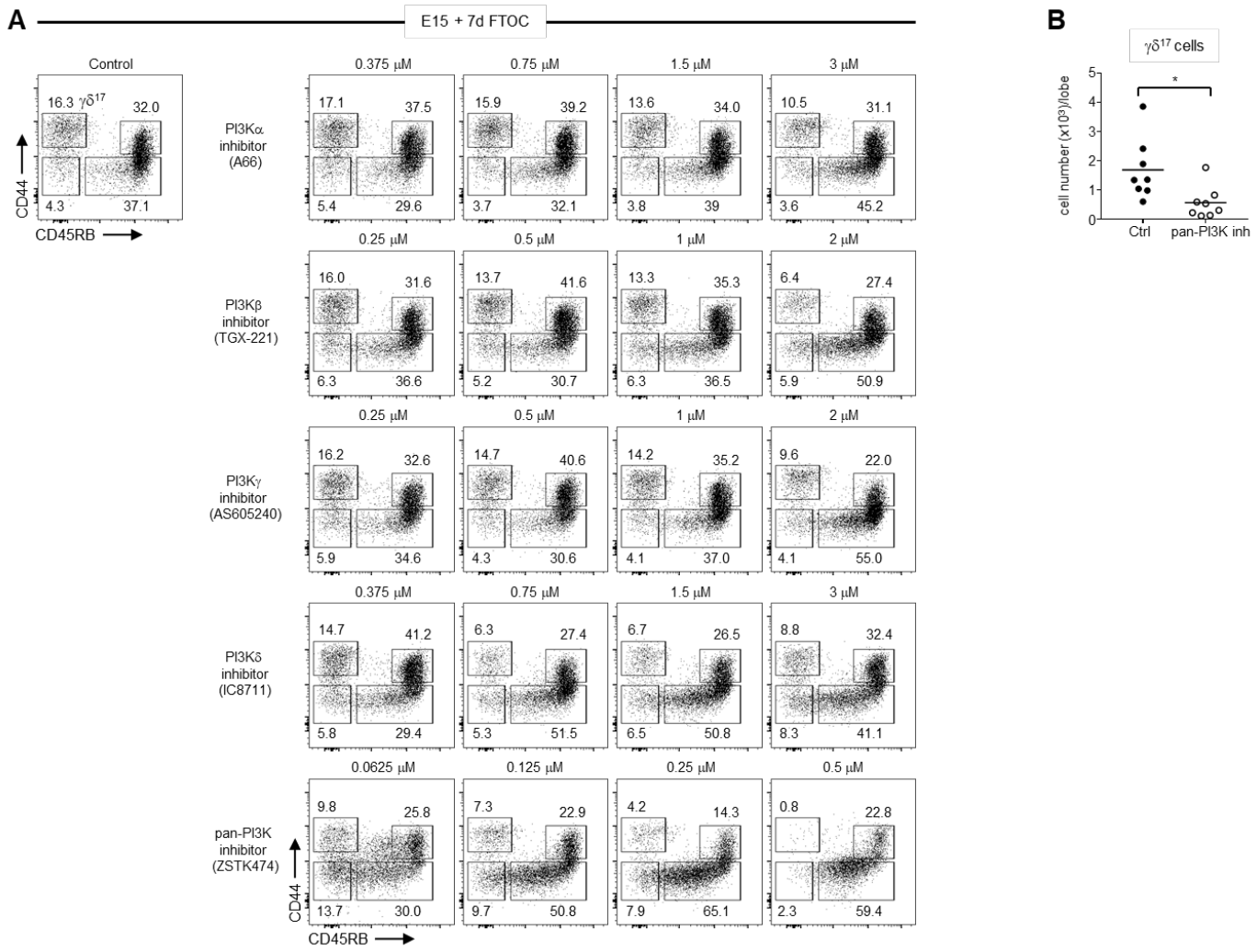

Fig. S5. γδ^{17} cell development requires PI3K activity. (**A**) Plots of γδ^{24-} T cells from 7-day FTOC of WT E15 thymic lobes in presence or absence of inhibitors (concentrations indicated) of PI3Kα (A66), PI3Kβ (TGX-221), PI3Kγ (AS605240), PI3Kδ (IC8711), or pan-PI3K inhibitor (ZSTK474). Percentages of gated cells are indicated on plots. (**B**) Summary graph shows absolute number of γδ^{17} cells from 7-day FTOC of WT E15 thymic lobes in presence or absence of a pan-PI3K inhibitor ZSTK474 (0.25 μM). Data are representative of two independent experiments. Each symbol represents at least 4 thymic lobes pooled. *$P \leq 0.05$ (Unpaired Student's *t*-test).

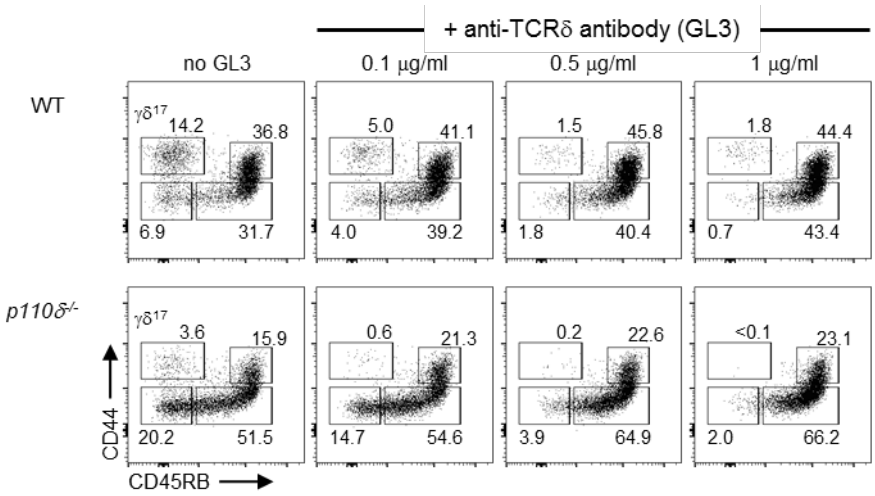

Fig. S6. TCRγδ signalling exacerbates loss of PI3K for γδ^{17} cell generation. Plots show γδ^{24-} T cells from 7-day FTOC of WT or *p110δ*$^{-/-}$ E15 thymic lobes in the presence or absence of anti-TCRδ antibody GL3 (concentrations indicated). Percentages of gated cells and γδ subset are indicated on plots.

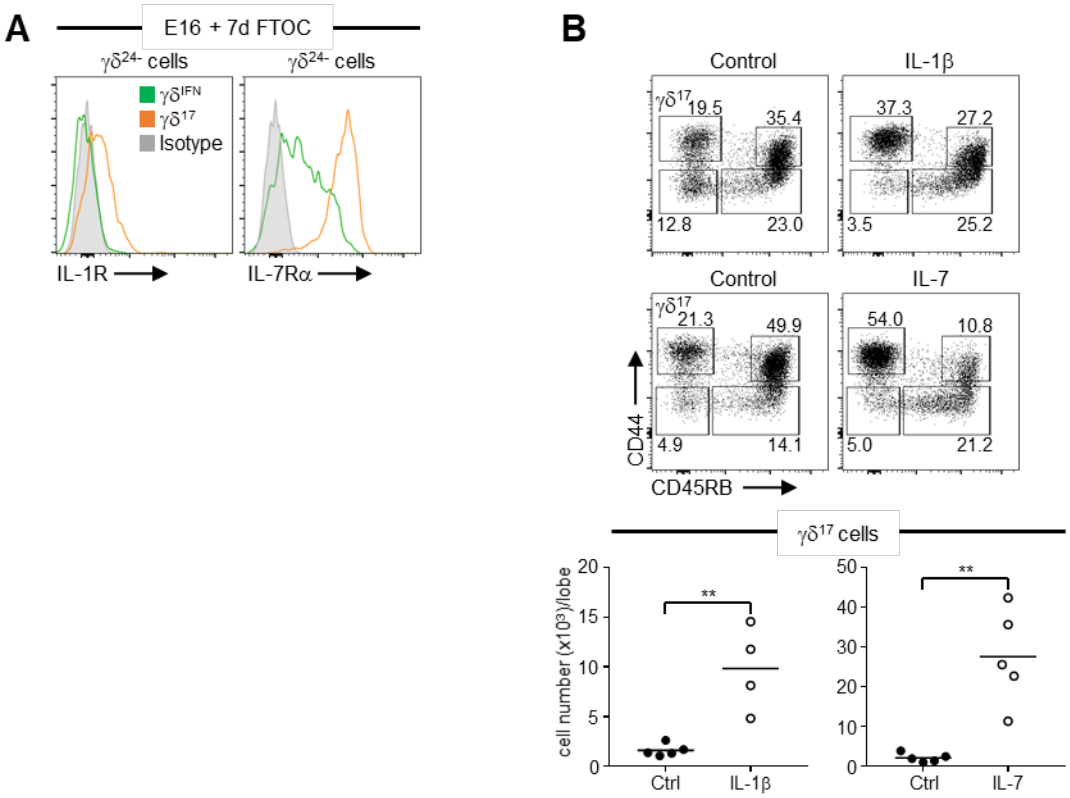

Fig. S7. γδ^{17} cells express elevated levels of IL-1R and IL-7Rα on their surface. (**A**) Histograms show expression of IL-1R and IL-7Rα on γδ^{IFN} (green) and γδ^{17} cells (orange) from 7-day FTOC of WT E16 thymic lobes. (**B**) Plots show γδ^{24-} T cells from 7-day FTOC of WT E15 thymic lobes in the presence or absence of IL-1β (5 ng/ml) or IL-7 (10 ng/ml). Percentages of gated cells and γδ subset are indicated on plots. Summary graphs show absolute number of γδ^{17} cells from associated cultures. Data are representative of two independent experiments. Each symbol represents at least 4 thymic lobes pooled. $^{**}P \leq 0.01$ (Unpaired Student's *t*-test).

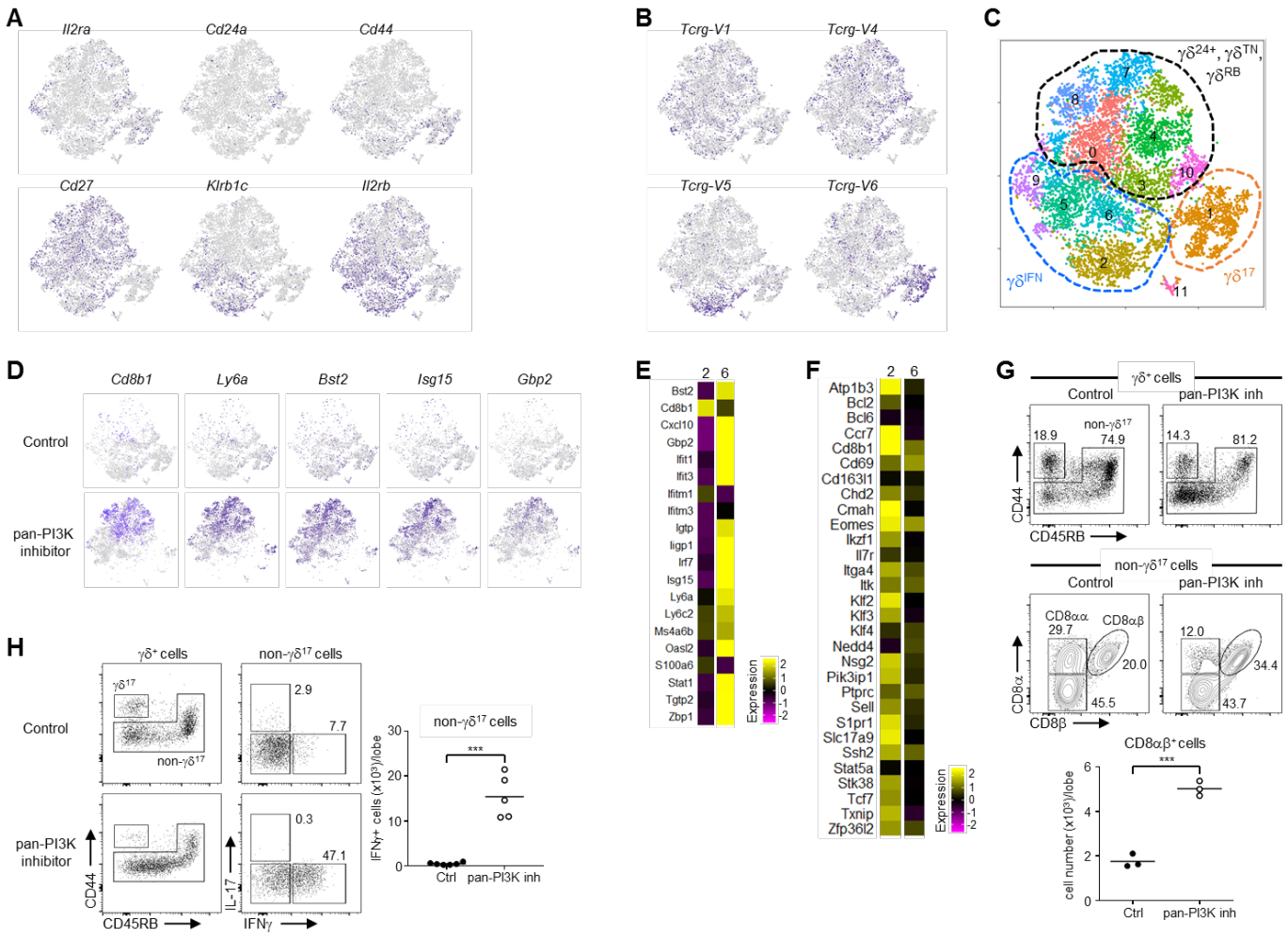

Fig. S8. Single-cell transcriptomic analysis of developing γδ T cells. (**A** and **B**) t-SNE representations show expression of known markers (**A**) and TCR-Vγ chains (**B**) used to identify distinct γδ subsets, in integrated γδ T cells from single-cell RNA-sequencing performed on sorted γδ T cells from 8-day FTOC of WT E15 thymic lobes in the presence or absence of pan-PI3K inhibitor ZSTK474 (0.25 μM). (**C**) t-SNE visualisation coloured and numbered by cluster after un-supervised clustering. Each dot represents a single cell. Demarcation (dashed line) of clusters correspond to a single or a group of γδ subsets as indicated. (**D**) t-SNE representations show expression of selected genes in control or PI3K inhibitor-treated γδ T cells. (**E** and **F**) Heatmaps show differentially expressed genes (DEGs) between cluster 2 and cluster 6 γδ T cells from untreated 8-day FTOC of WT E15 thymic lobes (adjusted $P \leq 0.05$). (**G**) Plots show γδ T cells from 5-day FTOC of WT E17 thymic lobes in the presence or absence of pan-PI3K inhibitor ZSTK474 (0.25 μM). Summary graph shows absolute number of CD8β$^+$ non-γδ^{17} cells. Each symbol represents at least 3 thymic lobes pooled. (**H**) Left panels show γδ T cells from 7-day FTOC of WT E15 thymic lobes in the presence or absence of pan-PI3K inhibitor ZSTK474 (0.25 μM). Right panels show intracellular staining for IL-17 and IFNγ in non-γδ^{17} cells after 3h stimulation ex vivo with PMA and ionomycin. Summary graph shows absolute number of IFNγ$^+$ non-γδ^{17} cells. Percentages of gated cells and γδ subset are indicated on plots. Data are representative of one (**A**-**G**) or three (**H**) independent experiments. Each symbol represents at least 4 thymic lobes pooled. ***$P \leq 0.001$ (Unpaired Student's *t*-test).

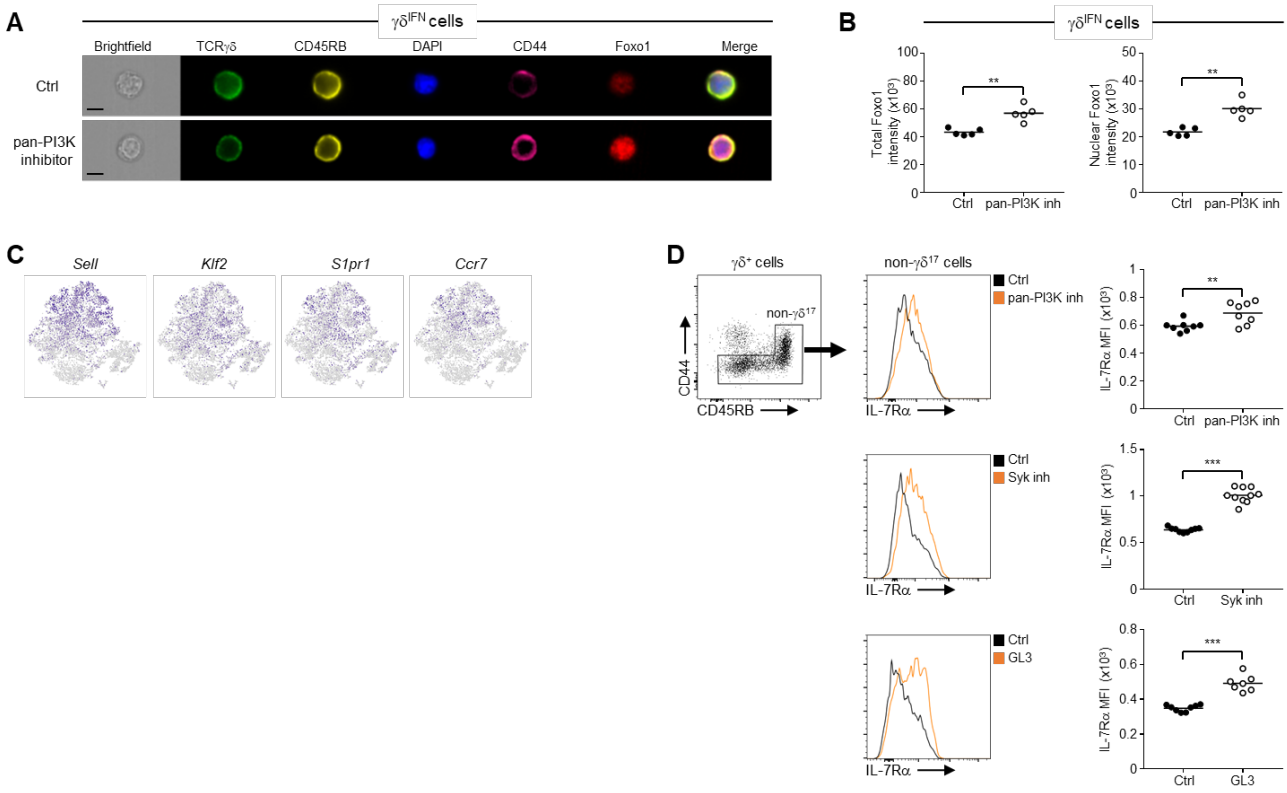

Fig. S9. PI3K inhibition upregulates Foxo1 activity in γδ^{IFN} cells. (**A**) Imagestream analysis of γδ^{IFN} cells from 7-day FTOC of WT E15 thymic lobes in the presence or absence of pan-PI3K inhibitor ZSTK474 (0.25 μM). Scale bar, 7 μm. (**B**) Summary graph shows total (left) and nuclear (right) Foxo1 intensity in γδ^{IFN} cells from experiments described in (A). Data are representative of two independent experiments. (**C**) t-SNE representations show expression of Foxo1 target genes in integrated visualisation of γδ T cells from 8-day FTOC of WT E15 thymic lobes in the presence or absence of pan-PI3K inhibitor ZSTK474 (0.25 μM). (**D**) Histograms (middle panels) show expression of IL-7Rα on non-γδ^{17} cells (from left panel) from 6-day FTOC of RORγt-GFP$^{+/-}$ E15 thymic lobes in the absence or presence of pan-PI3K inhibitor ZSTK474 (0.25 μM), Syk inhibitor BAY61-3606 (0.4 μM), or GL3 (1 μg/ml). Summary graphs show MFI of IL-7Rα in non-γδ^{17} cells from the different treatments. Data are representative of two independent experiments. Each symbol represents at least 4 thymic lobes pooled. $^{**}P \leq 0.01$ and $^{***}P \leq 0.001$ (Unpaired Student's *t*-test).

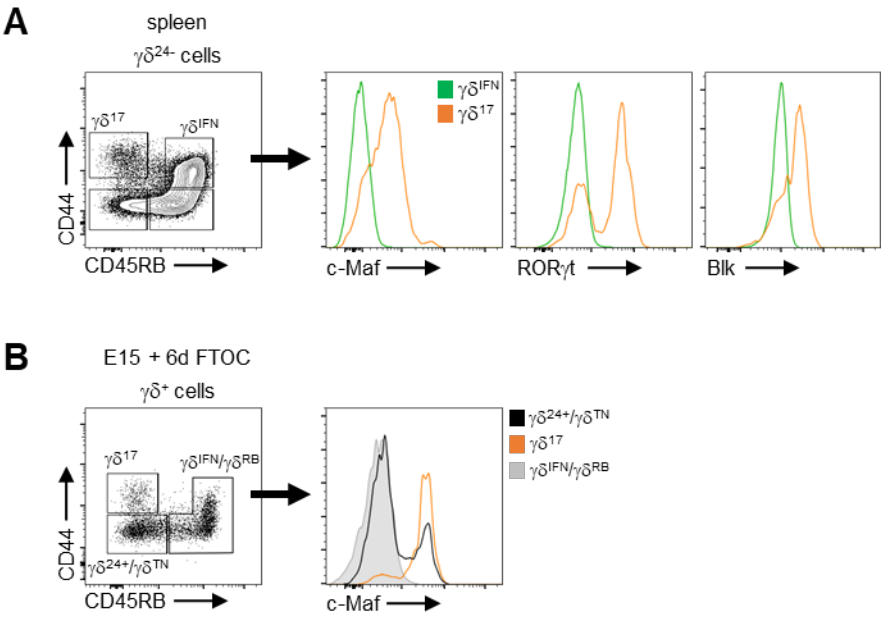

Fig. S10. Expression of IL-17-associated transcription factors in distinct γδ subsets. (**A**) Histograms show expression of c-Maf, RORγt and Blk in peripheral $\gamma\delta^{IFN}$ and $\gamma\delta^{17}$ cells from spleen of adult WT mice. (**B**) Histogram shows expression of c-Maf in distinct γδ subsets from 6-day FTOC of WT E15 thymic lobes. γδ subsets are indicated on the plots. Data are representative of two independent experiments.